https://ntrs.nasa.gov/search.jsp?R=19830013241 2020-03-21T03:35:40+00:00Z

General Disclaimer

One or more of the Following Statements may affect this Document

- This document has been reproduced from the best copy furnished by the organizational source. It is being released in the interest of making available as much information as possible.
- This document may contain data, which exceeds the sheet parameters. It was furnished in this condition by the organizational source and is the best copy available.
- This document may contain tone-on-tone or color graphs, charts and/or pictures, which have been reproduced in black and white.
- This document is paginated as submitted by the original source.
- Portions of this document are not fully legible due to the historical nature of some of the material. However, it is the best reproduction available from the original submission.

Produced by the NASA Center for Aerospace Information (CASI)

NASA-CR-167725
c.1

SPECTROLAB

FINAL REPORT

for

LARGE AREA, LOW COST SOLAR CELL DEVELOPMENT AND PRODUCTION READINESS

Prepared for:

NATIONAL AERONAUTICS AND SPACE ADMINISTRATION
JOHNSON SPACE CENTER
Houston, Texas 77058

Contract NAS9-16126

Prepared by:

D. Michaels

Approved by:

Nick Mardesich
Product Development Group Leader
Advanced Programs

SPECTROLAB, INC.
12500 Gladstone Avenue
Sylmar, California 91342

January, 1982

35067

(NASA-CR-170037) LARGE AREA, LOW COST SOLAR CELL DEVELOPMENT AND PRODUCTION READINESS Final Report (Spectrolab, Inc.) 60 p HC A04/MF A01 CSCL 10A

N83-21512

Unclas
G3/44 35067

TABLE OF CONTENTS (Cont'd)

Section		Page
3.6.2	Photolithographically Defined Contacts	24
3.6.2.1	Contact Strike Evaporation	24
3.6.2.2	Photomask Application	24
3.6.2.3	Etchback of Contact Strike	25
3.6.2.4	Photoresist Strip	29
3.6.2.5	Contact Plateup	32
3.6.2.6	Laser Sizing and Contact Metallization Sinter	33
3.7	Dual Antireflective Coating	35
3.8	Mechanical Wraparound Bonding	35
4.0	Cell Characteristics	38
4.1	Yield Data	38
4.1.1	Conventionally Contacted Cell Yield	38
4.1.2	Mechanical Wraparound Contact Cell Yield	41
4.2	Electrical Measurement Data	43
4.2.1	Conventional Contacts	43
4.2.2	Mechanical Wraparound Cells	43
4.3	Electron Irradiation Testing	48
4.4	Thermal Shock Testing	48
4.4.1	Conventionally Contacted Cells	48
4.4.2	Mechanical Wraparound Contacted Cells	51
4.5	Humidity Resistance Testing	51
4.5.1	Conventionally Contacted Cells	51
4.5.2	Mechanical Wraparound Contacted Cells	53
5.0	Recommendations	56
6.0	Summary	57

1.0 INTRODUCTION

The goal of the PEP Solar Cell Development program has been to develop a process sequence for a large area ($\geq$ 25 cm^2) silicon solar cell that is achievable in a mechanized or semiautomated manufacturing facility. An option wraparound contact process, while increasing the cost of the device somewhat, can reduce the overall cost of the panel by making possible a higher degree of automation in panel manufacturing.

This large area cell will be incorporated into the Power Extension Package, an optional power unit designed to extend the duration of space shuttle missions. This 25 kW, deployable array will operate in a low radiation regime that will subject it to approximately 3×10^{14} 1 MeV electrons/cm^2 over the lifetime of the unit.

Generic cell choice was guided by the expected electron fluence, by the packing factors of various cell envelope designs onto each panel to provide needed voltage as well as current, by the weight constraints on the system and especially by the cost goals of the contract. A goal of $30/watt demands reduced handling per watt of power (i.e., large area devices) as well as reduced handling per piece (i.e., mechanized facility).

2.0 BACKGROUND

2.1 LARGE AREA BLANKS

Several lines of attack were studied to effect reduction in cost per watt. The scaleup in cell area will effect savings at cell filtering and cell lay-down at panel level by reducing handling per area. The truncated square cell envelope of the final design also effects some savings in silicon usage by optimizing area used from a three inch round wafer. The area of the final device was approximately 34.4 cm^2.

2.2 PROCESS SEQUENCE

The process sequence developed lends itself to a mechanized line which would reduce manpower needs and therefore cost. Many of the techniques applied are used widely in the semiconductor industry, such as screen printing, infrared belt alloy, and photolithography and can be accomplished on standard equipment. A three or four inch round silicon blank fits standard automatic cassette loading and handling equipment.

2.3 GENERIC CELL CHOICES

The initial cell type chosen for the program was a 2 Ω-cm BSF cell which offers some advantages in efficiency and thermal control properties as well as fitting the mission radiation regime. The projected fluence over the unit's lifetime is $3 \cdot 10^{14}$ MeV electrons per cm^2. This cell was to be manufactured either with conventional contacts (for TRW) or wraparound contacts (for LMSC). The residual aluminum reflector formed simultaneously with the back surface field has shown a lower thermal alpha on 10 Ω-cm BSF cells than an evaporated aluminum reflector. Also

this reflector could withstand the printed dielectric sinter, as was shown on the HEWACS "High Efficiency Wraparound Contact Solar Cell"* the contracts under which the printed dielectric insulation was developed.

Later, based on the electron irradiation studies done at NASA-Lewis Research Center to aid generic cell choice, the two cell users requested baseline changes to a 10 Ω-cm BSF/BSR for the customer who preferred conventional contacts and a 2 Ω-cm BSR cell manufactured with a printed dielectric wraparound contact system for the customer preferring wraparound contacts. Also, a baseline change from metal shadow masking to photolithography was made for contact definition, to provide more flexible contact patterns.

2.4 PRINTED DIELECTRIC WRAPAROUND CONTACT CELLS

Due to the baseline change, the dielectric insulation technique developed for a high efficiency, i.e., BSF cell, was applied for the first time to a cell with an evaporated BSR and without a field. Difficulty was encountered in obtaining good adherence of the dielectric to the BSR and in developing contact strike etch back techniques that would remove the Cr-Pd-Ag contacting system but not attack the insulation or photoresist.

The adhesion of the dielectric was improved and its tendency to craze reduced by several process changes; however, the Cr-Pd-Ag contact system used with the dielectric presented an insurmountable problem in contact etchback given existing schedules and funding. Also, the additional projected cell cost attributable to the wraparound processing was becoming unacceptable.

---

*NAS3-20035, NAS3-21270

2.5 MECHANICAL WRAPAROUND CONTACT CELLS

A design change to a mechanical wraparound was made by mutual agreement between Lockheed Space and Missile Company and NASA-Johnson Space Flight Center. The agreed-upon configuration utilizes an interconnect bonded to the back of the cell and welded to the front contact. A modified acrylic-kapton-acrylic prelaminated sandwich is used as the bonding/insulating material. Currently a 1 mil silver ribbon forms the wrapped "N" interconnect. Such a process is not sensitive to generic cell type as the dielectric wraparound technique appeared to be.

2.6 FINAL DEVICE CONFIGURATIONS

The final cell envelope and contact patterns evolved in conjunction with the respective cell users appear in Figures 1 and 2. These contact patterns were designed to optimize collection efficiency while reducing active area shadowing and also meeting interconnect pad requirements of each respective customer. Further iteration is possible with both contact designs.

Figure 1

ORIGINAL PAGE IS
OF POOR QUALITY

CONVENTIONAL CONTACT PEP CELL
10 Ω-cm BSF/BSR

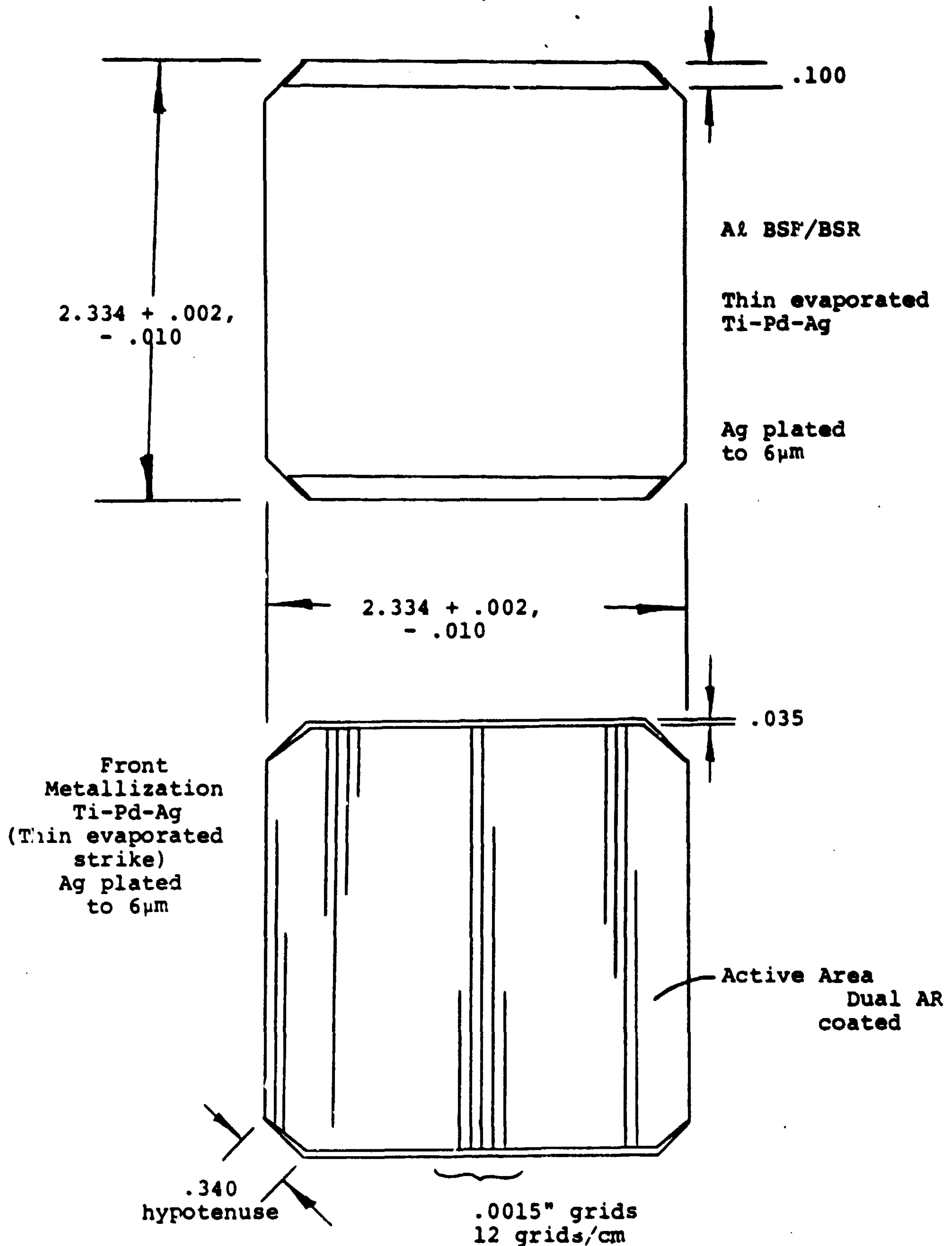

All Dimensions in Inches
Unless Otherwise Noted

Figure 2

MECHANICAL W/A CONTACT PEP CELL
2 Ω-cm BSR

ORIGINAL PAGE IS
OF POOR QUALITY

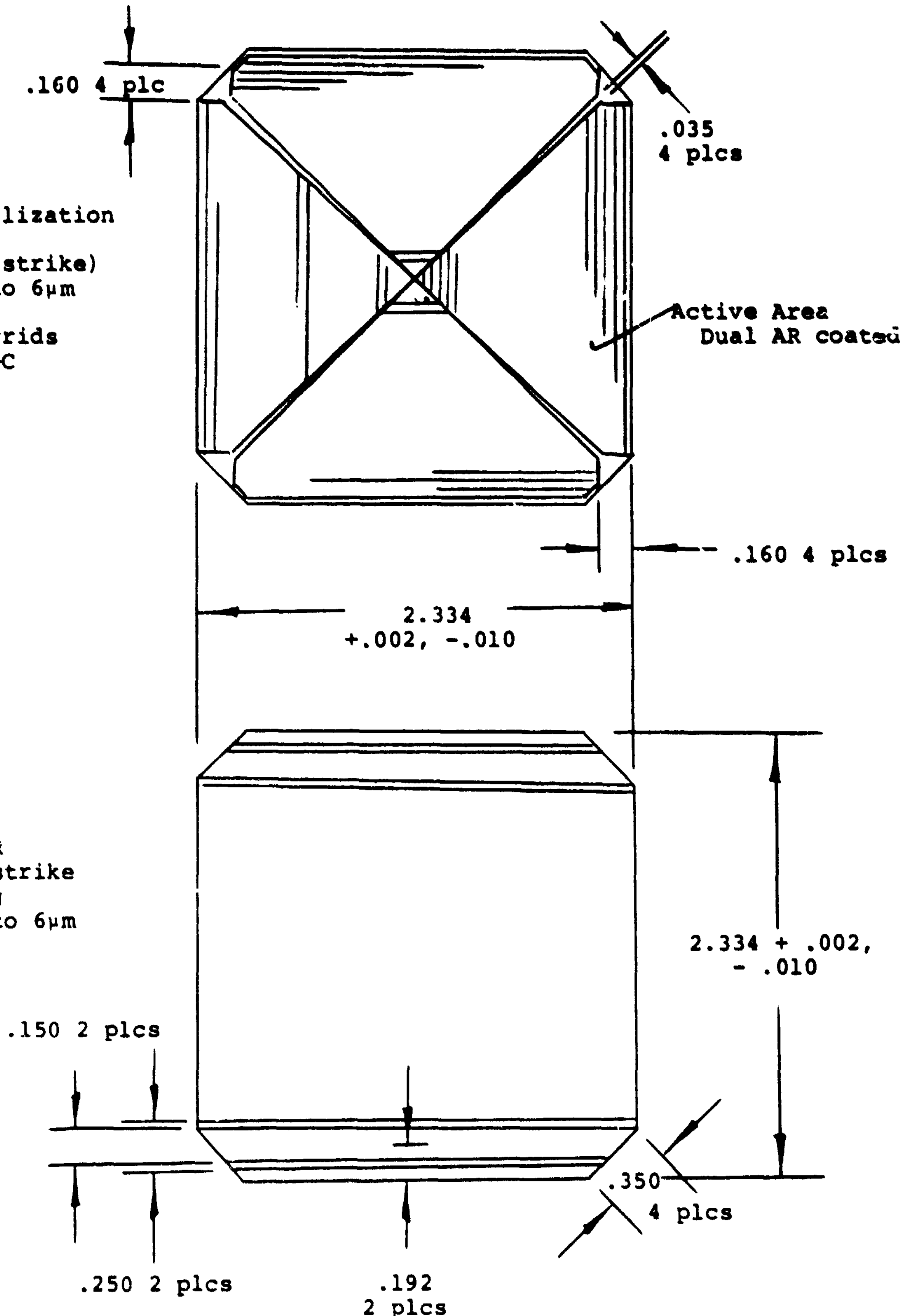

All Dimensions in Inches
Unless Otherwise Noted

3.0 PROCESS EVOLUTION

3.1 BASELINE PROCESS SEQUENCES

3.1.1 Initial Baseline Process Sequence

The initial baseline process sequence showing both contact types appears in Figure 3. This sequence is similar to processing carried out on small area printed dielectric wraparound cells. The dielectric application steps are omitted on the conventional contact cell and a Ti-Pd-Ag contact system replaces the Cr-Pd-Ag combination used with the dielectric insulation.

3.1.2 Reconfigured Cell Baseline Process Sequence

The change of generic cell choice at the February 1981 PEP Design Review changed both some process steps and some of the order of processes. Evaporation through metal shadow masks was replaced by contact strike evaporation/photomask application/contract strike etchback/contact plateup. Reconfiguring of the wraparound cell design relocated the wrap areas of the contact to the polished edges of the wafer enabling the cell sizing steps to wait until the end. The BSF formation was replaced by a back etch step and a subsequent aluminum BSR evaporation. The contact application and definition showed the greatest changes for both cell types. See Figures 4 and 5 for these process sequences. A Ti-Pd-Ag etchback was in use at Spectrolab but a workable etchback for the Cr-Pd-Ag contacts was not known, necessitating some investigation.

3.1.3 Mechanical Wraparound Cell Process

When difficulties were not resolved in the dielectric contact processing, an alternative method of forming a wraparound

Figure 3

INITIAL BASELINE CELL PROCESS SEQUENCE

ORIGINAL PAGE IS
OF POOR QUALITY

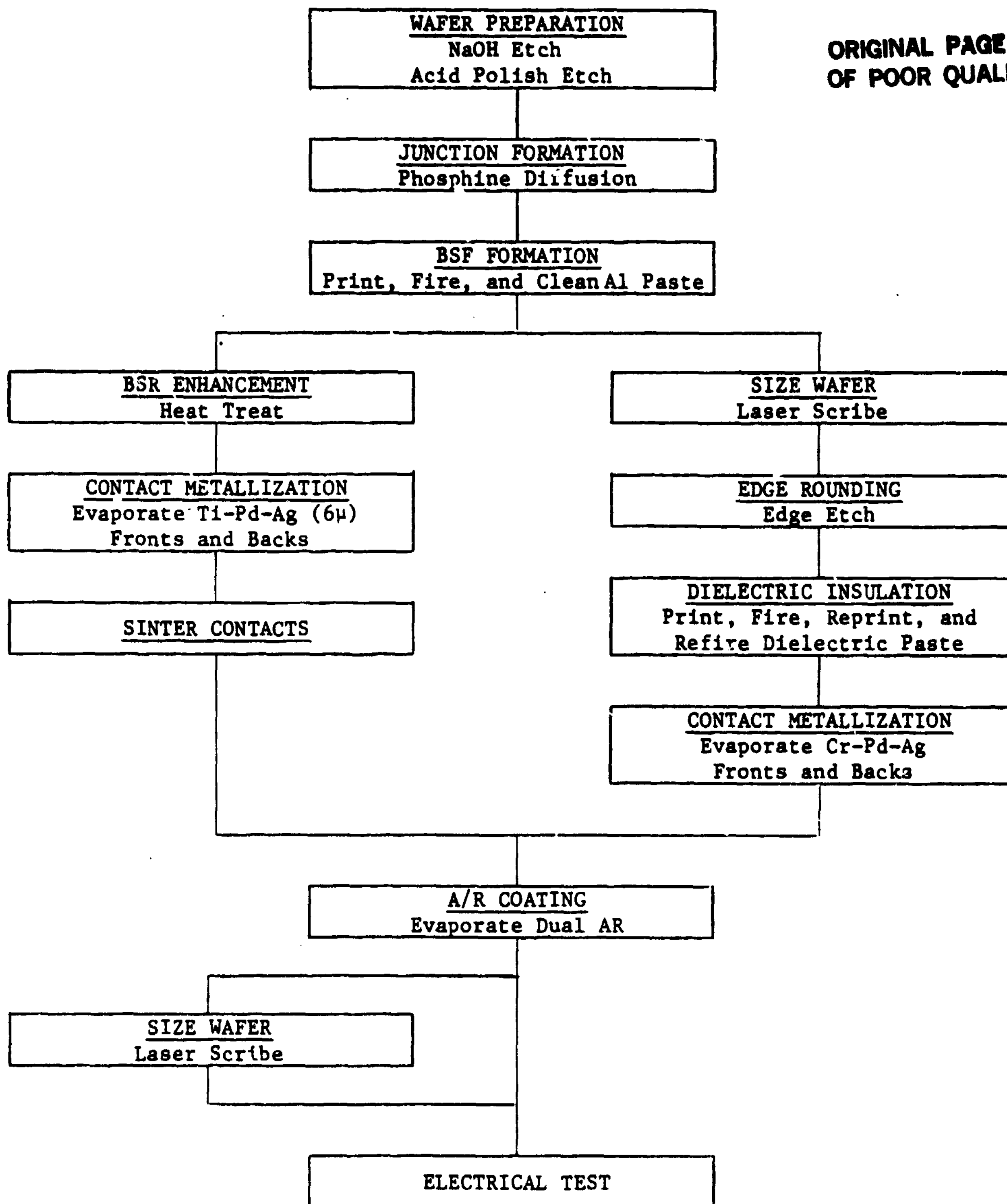

Figure 4

RECONFIGURED BASELINE PROCESS SEQUENCE
CONVENTIONALLY CONTACTED CELL

ORIGINAL PAGE IS
OF POOR QUALITY

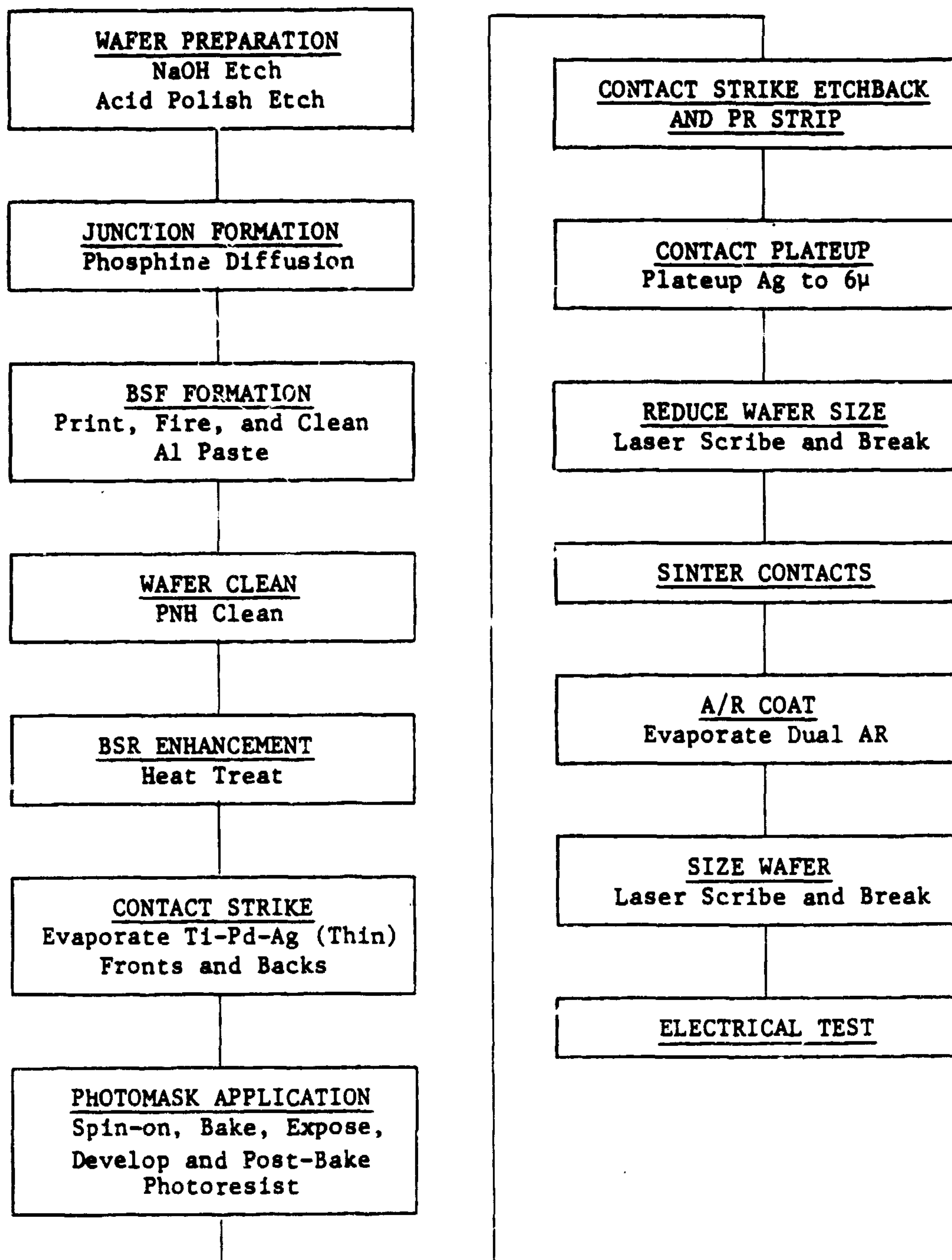

ORIGINAL PAGE IS
OF POOR QUALITY

Figure 5

RECONFIGURED BASELINE PROCESS SEQUENCE
DIELECTRIC WRAPAROUND CONTACTED CELL

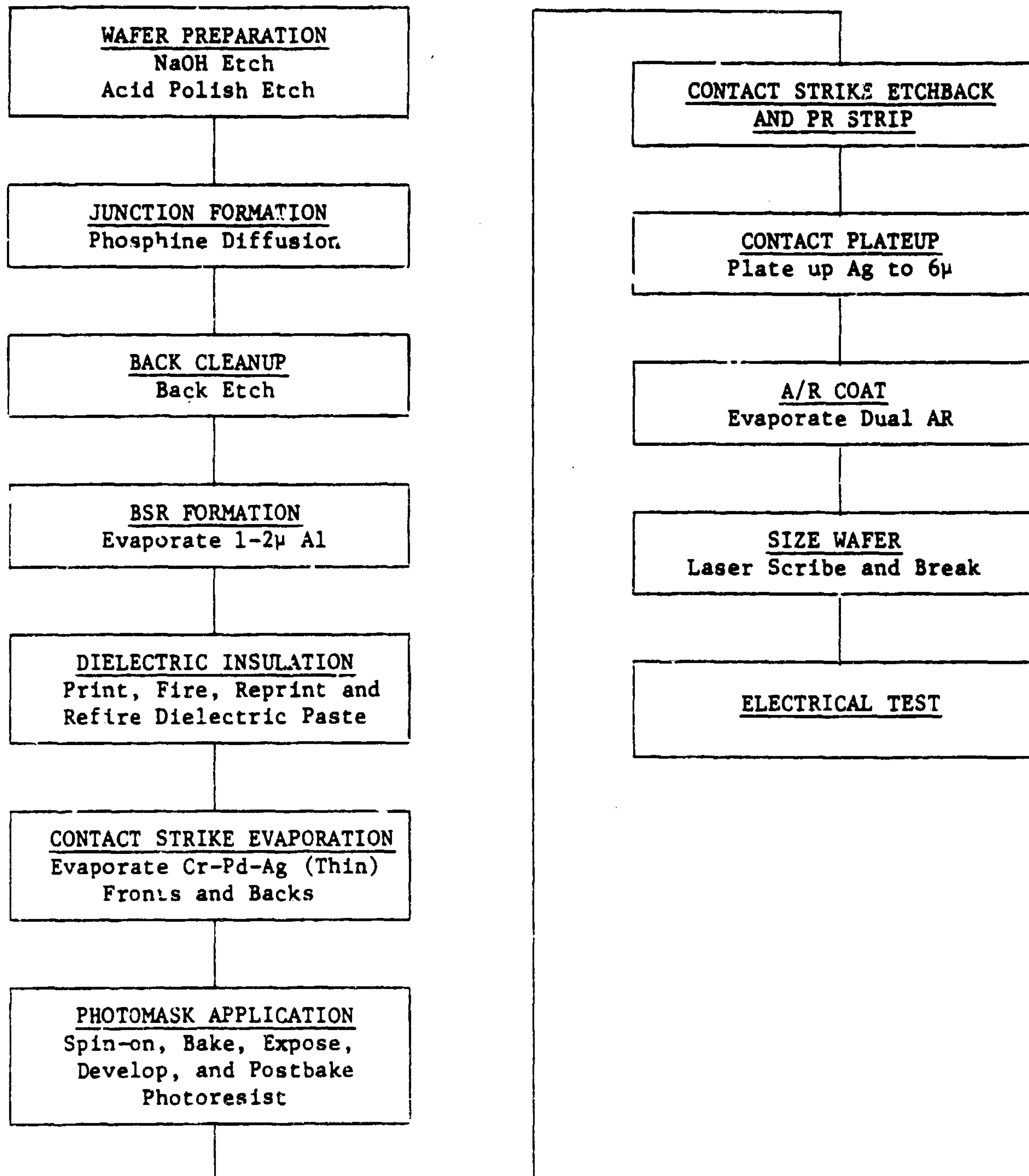

contact was suggested and fifteen large area cells using this technique were fabricated for evaluation by LMSC. A bond/insulating material attaches an interconnect to the cell back and the interconnect wraps around the cell edge and is welded. The bonding material being used is a modified acrylic/kapton/modified acrylic prelaminate, each layer in a .001" thickness material, which is microspot resistance welded in the four corners to the front of the cell. The front contact pattern was redesigned to incorporate weld pad areas in the four corners and also to improve current collection.

3.2 WAFER PREPARATION

The baseline wafer preparation consisted of a concentrated sodium hydroxide etch to remove saw damage from wafer slicing followed by an acid etch which results in a polished but slightly "pillowed" surface. The acid etch was omitted for several reasons:

1) Acid polishing sometimes leaves etch "stains" which are really a series of small etch pits. These pits, when located on the active area, tended to plate full of silver during later processing. The silver did not adhere well but would not readily rinse off and necessitated rubbing to remove it.

2) The acid polish step is done on loose wafers and is difficult to mechanize. Wafers acid etched in a cassette develop "boat marks" or uneven etching where wafer edges are held in cassette slots. Therefore the step does not fit well in a mechanized facility.

3) Chemicals used for the etch are more expensive than basic etchants.

4) The pillowed surface resulting from NaOH etching for a sufficient time is not excessively rougher than an acid polished surface.

The acid polish etch was omitted after TRW Lot 3 (i.e. Lot 4 was NaOH etched only). All LMSC cells were NaOH etched only.

3.3 JUNCTION FORMATION

Junction formation is accomplished by the standard phosphine diffusion in a tube furnace. Junctions on the original cells utilized a 40 Ω/□ sheet resistivity to match the stainless steel metal masks chosen (see Section 3.6.1).

When the design change moved the contact definition to photoresist and the metal shadow masking was avoided, shallow junctions (100-120 Ω/□ sheet resistivity) could be used with the fine-line grids achievable with photolithography.

3.4 BACK SURFACE FIELD FORMATION

3.4.1 Tube Furnace Alloy

The baseline BSF formation utilized an aluminum paste (Engelhard A-3484) screen printed onto the back surface of wafers as a P+ source. After the paste screening vehicle was dried off in a forced air oven, the wafers were loaded into a quartz boat and alloyed for a short time in a tube furnace with a controlled atmosphere.

Using the initial silicon blanks of 2 Ω-cm resistivity, a matrix of firing times and oven temperatures was run. These large wafers were diced to 2 x 4 cm size for contact evaporation since the hard metal tooling for the large cells had not arrived.

These cells showed curve shapes in the range of .70-.73, below that which was expected (.76-.78). Also, open circuit voltages were not as high as expected. An analysis of the light and the dark derived I-V curves indicated a front end n+ junction contamination rather than an unoptimized BSF. It was theorized that a BSR enhancement step done later at an elevated temperature was driving in contamination remaining after excess paste cleanup. The aluminum particles remaining after firing can be washed around to the wafer fronts during paste cleanup and are difficult to clean off by rinsing step alone. Addition of a stringent cleaning step (PNH clean) between paste cleanup and the BSR enhancement step improved cell performance to expected values.

When the cell choices were finalized, a reoptimization of alloy parameters was run on the 10 Ω-cm base resistivity yielding the following matrix of voltage probes. See Figures 6 and 7. Data from a completed lot of cells is given in Table 1. The 10 Ω-cm BSF cell processing also included the PNH clean.

3.4.2 Infrared Belt Alloy of BSF

In keeping with the goal of a low cost, mechanizable cell process sequence, a lot of cells was run through the IR belt furnace. Parameters used were previously obtained on an optimization run of 10 Ω-cm, 1.7 x 1.7 cm square blanks and the same paste type. Results for the completed lot of cells are in Table 2.

3.4.3 Past Formulation Change

The back surface field was successfully produced on several lots of cells using the infrared belt furnace but the back side of the cells had a rough surface. This may have been caused by incomplete bakeout of the screening vehicle from the proprietary Engelhard formula. Accordingly, a change was made to an in-house formulation

ORIGINAL PAGE IS
OF POOR QUALITY

Figure 6

10 Ω-cm TUBE FIRED SCREEN PRINTED Al

Alloyed for 30 seconds

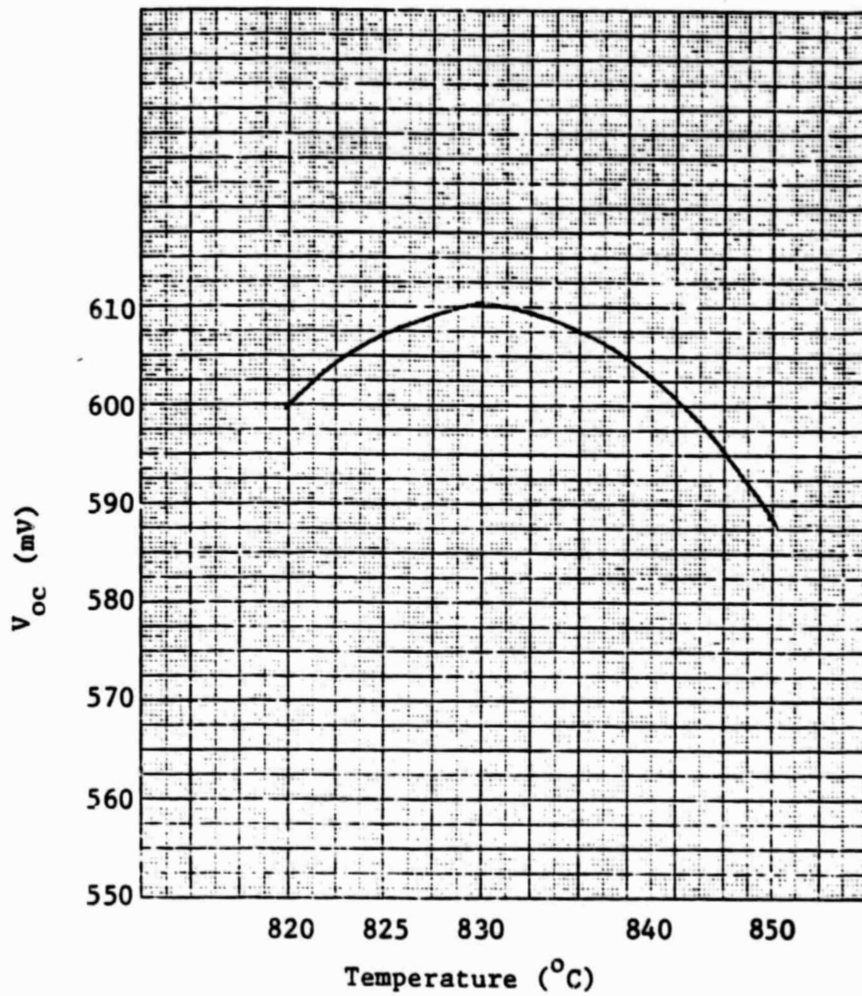

Figure 7

10 Ω-cm TUBE FIRED SCREEN PRINTED Al

Alloyed at 830°C

ORIGINAL PAGE IS OF POOR QUALITY

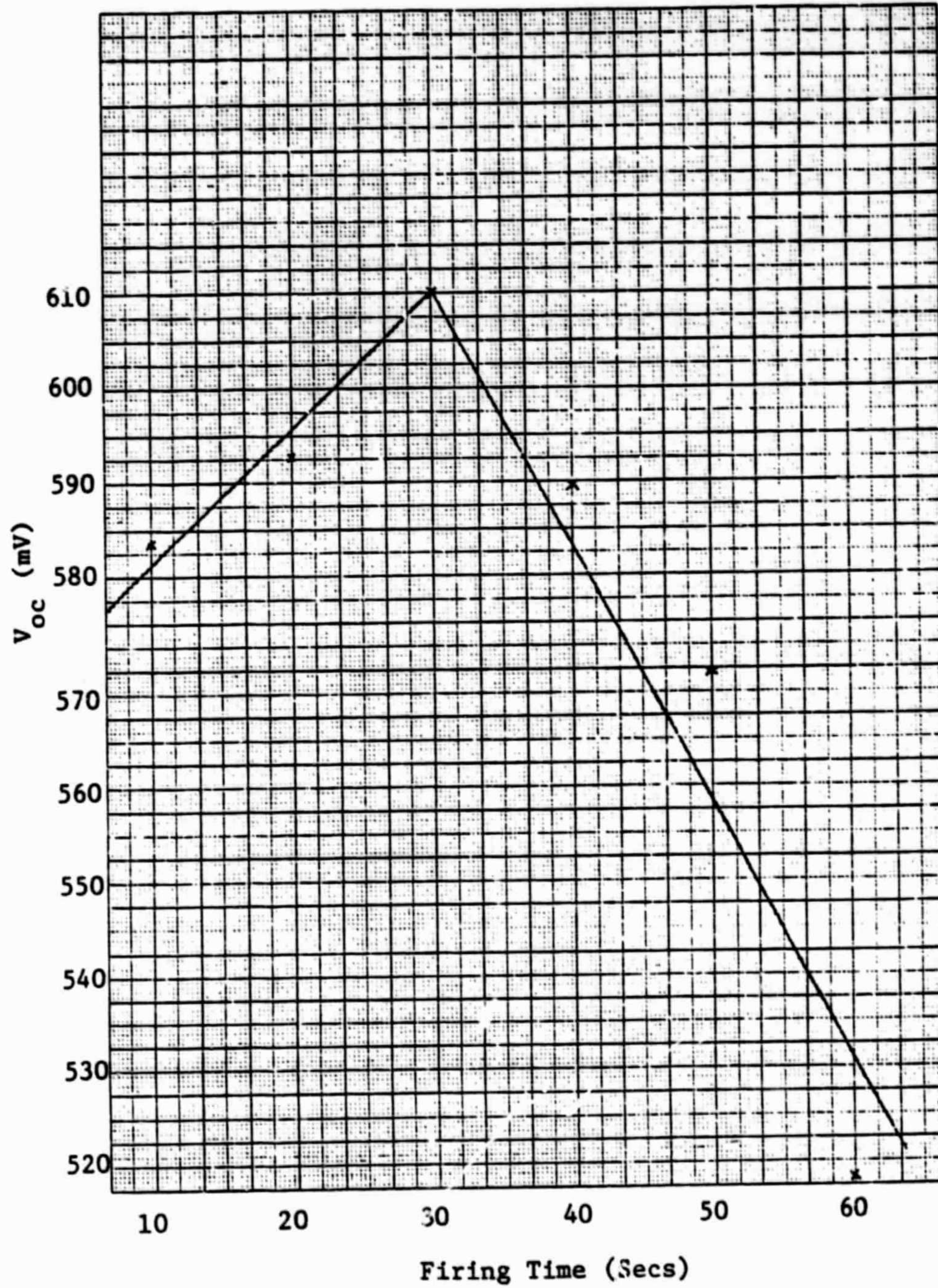

ORIGINAL PAGE IS
OF POOR QUALITY

Table 1

10 Ω-cm BSF, RESIDUAL ALUMINUM BSR
ALLOYED IN TUBE FURNACE
5.9 x 5.9 cm x .008 INCH, DUAL AR CELLS

	V_{oc} mV	I_{sc} mA	V_{mp} mV	I_{mp} mA	P_{max} mW	CFF	η %
Lot 3							
3-1	605	1427	495	1300	.6435	.745	13.8
3-2	603	1420	500	1300	.6500	.759	14.0
3-3	608	1420	505	1320	.6666	.772	14.3
3-4	605	1430	504	1327	.6688	.773	14.4
3-5	605	1480	493	1366	.6734	.752	14.5
3-6	612	1475	514	1380	.7093	.786	15.2
3-8	603	1435	505	1345	.6792	.785	14.6
3-9	612	1400	510	1305	.6656	.777	14.3
3-10	610	1405	508	1305	.6629	.774	14.2
3-11	613	1440	515	1325	.6824	.773	14.7
3-12	618	1510	509	1390	.7075	.758	15.2
3-13	615	1466	507	1380	.6997	.776	15.0
3-14	605	1455	502	1370	.6877	.781	14.8
3-15	608	1490	505	1390	.7020	.775	15.1
3-16	605	1410	508	1300	.6604	.774	14.2
3-17	605	1440	505	1335	.6742	.774	14.5
3-19	605	1450	508	1310	.6656	.759	14.3
3-20	610	1460	508	1380	.7010	.787	15.1
Average	608.2	1445	505.6	1340	.6778	.771	14.57

Tested at AM0, 28°C

ORIGINAL PAGE IS
OF POOR QUALITY

Table 2

PEP 10Ω-cm BSF/BSR SOLAR CELL ALLOYED IN IR FURNACE

	V_{oc} mV	I_{sc} mA	V_{mp} mV	I_{mp} mA	P_{max} mW	CFF	η %
Lot 4							
4A-1	609	1460	504	1375	.6930	.779	14.9
4A-2	607	1450	498	1305	.6499	.738	14.0
4A-3	600	1425	492	1335	.6667	.780	14.3
4A-4	600	1440	504	1320	.6653	.770	14.3
4A-5	607	1465	500	1345	.6725	.756	14.4
4A-6	603	1435	503	1340	.6740	.779	14.5
4A-7	598	1425	501	1320	.6613	.776	14.2
4B-1	610	1440	512	1345	.6886	.784	14.8
4B-2	608	1415	513	1320	.6772	.787	14.6
4B-3	605	1425	503	1300	.6539	.758	14.1
4B-4	608	1455	502	1345	.6572	.763	14.1
4B-5	607	1440	502	1280	.6426	.735	13.8
4B-6	607	1445	512	1340	.6861	.782	14.7
Average	605.3	1440	503.5	1328	.6683	.768	14.4

Tested at AM0, 28°C

which was developed by extensive research on terrestrial cells. Thick Film Systems fabricated the paste to our formula using a high purity aluminum powder. The cells processed with this paste had a markedly smoother back surface, possibly due to the cleaner driving off of the screen vehicle. Also, the paste cleanup was much easier resulting in fewer broken cells (3% vs. 6.5% broken for the Engelhard paste). The aluminum oxide layer remaining after alloy was less tenaceous.

3.4.4 BSR Enhancement Step

A heating cycle used to enhance the reflectivity of the residual layer of aluminum was initially done after the paste cleanup and a cleaning step. It was hoped that performing the "heat treatment" before the paste cleanup would avoid placing a contaminated wafer in a high temperature environment. Thus the PNH clean, which necessitated protecting the aluminum layer with an ink mask, could be avoided. A lot of cells using this altered process showed satisfactory electrical output results. See Table 3.

3.5 PRINTED DIELECTRIC INSULATION

3.5.1 Adherence to Evaporated Aluminum BSR

A lot of 2 Ω-cm BSR cells was evaporated with a 1-2μ aluminum reflector and had the dielectric layers screen printed and sintered. The dielectric layers delaminated during a tape peel test at this point from two of three cells. Visual examination of the BSR under 400X magnification revealed a less-than-optimum surface condition of the BSR. The aluminum showed some particulate matter embedded in the reflector on the cells that had delaminated insulation. A cleaning step to remove this foreign matter was inserted after BSR evaporation and before dielectric print. A one-minute dip in dilute hydrochloric acid removed a small

ORIGINAL PAGE IS
OF POOR QUALITY

Table 3

PEP 10 Ω-cm BSF/BSR SOLAR CELLS ALLOYED IN IR FURNACE

Tested at 28°C, AM0

Lot-Cell	V_{oc} mV	I_{sc} mA	V_{mp} mV	I_{mp} mA	P_{max} mW	CFF	Eff. %
6-1	603	1450	491	1340	.6579	.752	14.1
6-2	607	1440	473	1325	.6267	.717	13.5
6-3	607	1455	500	1350	.6750	.764	14.5
6-4	604	1460	498	1310	.6524	.743	14.0
6-5	601	1460	493	1365	.6729	.767	14.5
6-6	602	1455	491	1385	.6800	.776	14.6
6-7	604	1435	496	1340	.6646	.764	14.3
6-8	606	1465	500	1350	.6750	.760	14.5
6-9	607	1455	494	1335	.6595	.747	14.2
6-10	607	1440	496	1345	.6671	.763	14.3
6-11	608	1440	494	1220	.6027	.688	13.0
6-12	606	1450	500	1360	.6800	.774	14.6
6-13	608	1450	505	1350	.6818	.773	14.6
6-14	604	1440	476	1335	.6355	.731	13.7
Avg.	605.3	1450	493.4	1336	.6594	.751	14.2

amount of the BSR and left a much cleaner back. The wafers thus treated had improved adherence between the dielectric and the aluminum.

3.5.2 Crazing of Dielectric Layers

Although dielectric adherence was improved, a larger than acceptable amount of crazing was occurring in the dielectric layers due to the thermal mismatch between the dielectric and the silicon. An experiment was designed to determine whether the aluminum BSR thickness was an important parameter which could reduce the effect of thermal mismatch. Wraparound dielectric pads were applied to 2 cm x 4 cm wafers to facilitate quick results (HEWAC Alternate Back Contact Configuration tooling was used). These wafers had 1.6, 2.5, 3.2, 7.3 and 12.8μ of evaporated aluminum reflector thickness. The 7.3μ layer showed the least amount of crazing - 50% of the cells showed no cracks; these cells also passed a tape peel test. This thickness of aluminum is comparable to the thickness of a residual aluminum layer.

3.5.3 Post-Sinter Anneal of Dielectric Layers

As a result of conversations with the manufacturers of the dielectric paste (TFS-126 RCB), Thick Film Systems, and also with Spectrolab's technical staff, an annealing step was added to the sinter cycle. Cells were held at a 500°C zone for 10 minutes as they were being withdrawn from the 575°C zone of a tube furnace. A number of 2 cm x 4 cm wafers processed with this anneal step showed only 10% loss due to crazing. Some of the wafers experienced ten cycles of thermal shock from -196°C to +100°C with no apparent cracking occurring.

3.5.4 Dielectric Sinter Time Lengthened

The large, 3" round, printed dielectric wafers first processed with the above process modifications pointed out the need for

Figure 8A

PRINTED DIELECTRIC WRAPAROUND CELL

ORIGINAL PAGE IS
OF POOR QUALITY

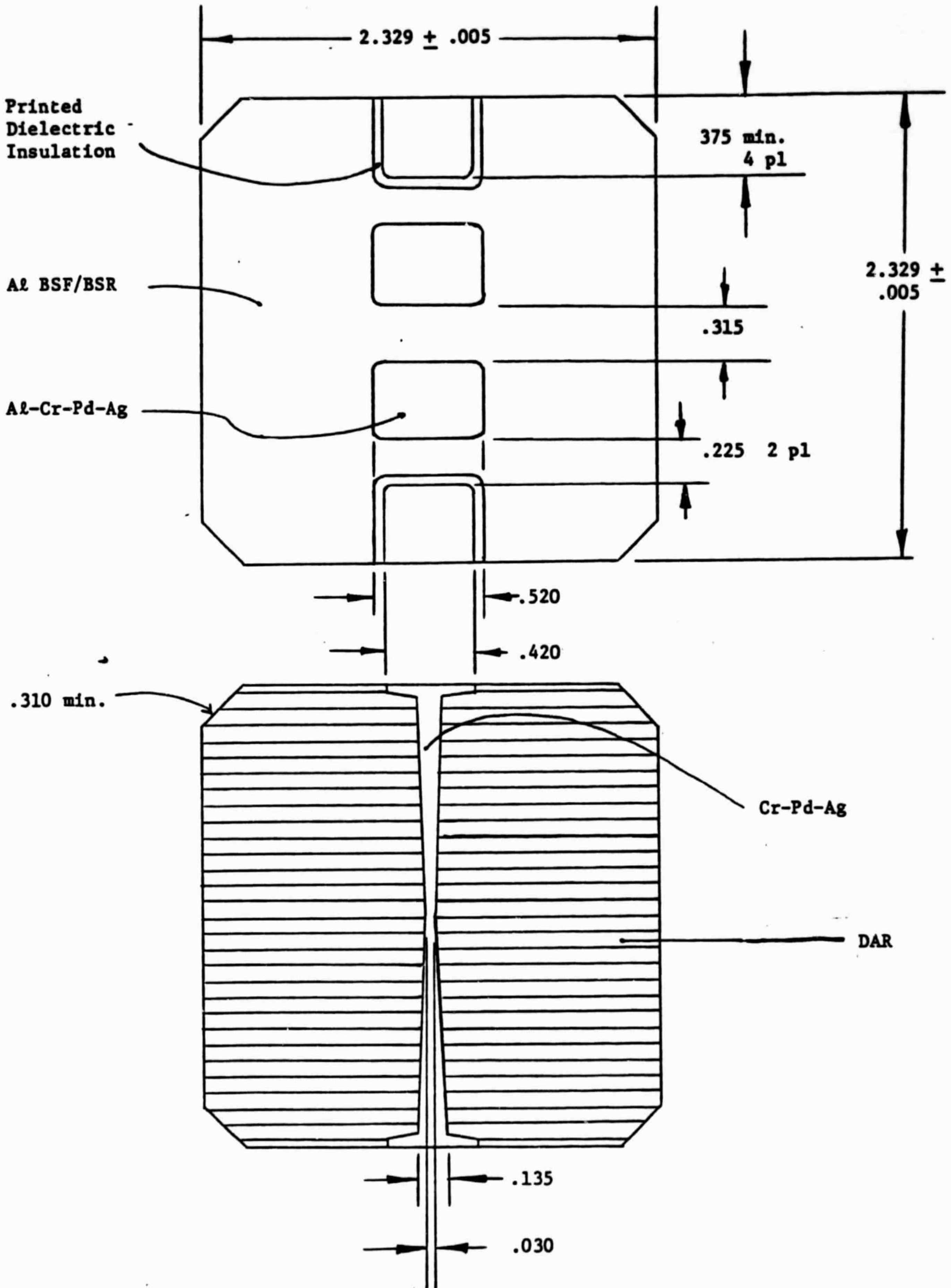

ORIGINAL PAGE IS
OF POOR QUALITY

Figure 8B

2 Ω-cm BSF CONVENTIONAL CONTACT CELL

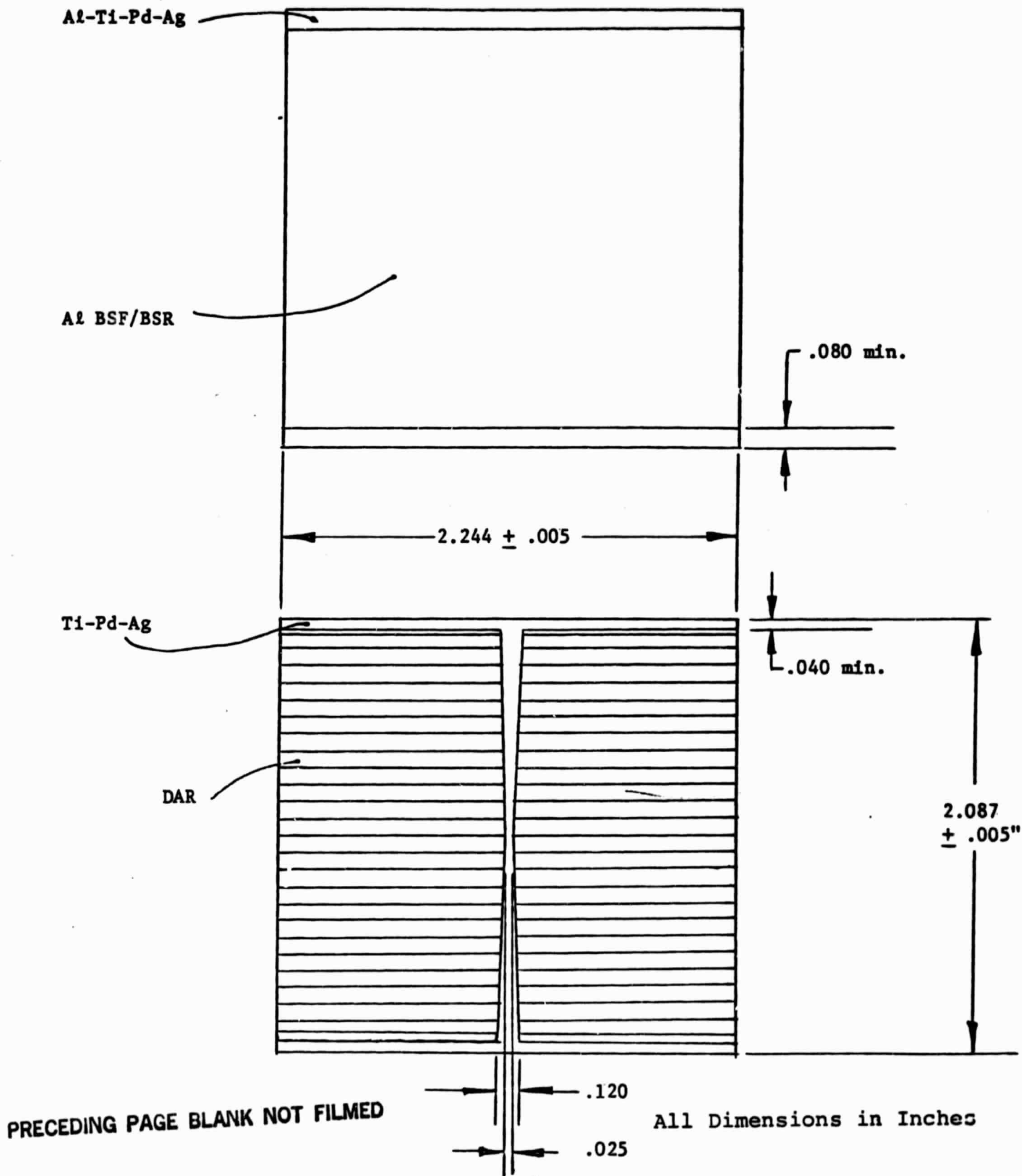

PRECEDING PAGE BLANK NOT FILMED

All Dimensions in Inches

3.6.2 Photolithographically Defined Contacts

A decision was made at the February 1981 PEP Design Review to change the baseline contact definition to photoresist masking techniques. The technique applied used an evaporated contact strike defined by etchback through a photoresist mask followed by plateup of silver onto the grid pattern. The subsequence of steps follows:

1) Contact Strike Evaporation
2) Photoresist Mask Application, Exposure and Development
3) Contact Strike Etchback
4) Photoresist Strip
5) Contact Plateup
6) Penumbra Etch
7) Laser Scribe to Size
8) Contact Sinter

Discussion of each step follows:

3.6.2.1 Contact Strike Evaporation

A contact strike of 800Å titanium for TRW cells or 800Å chromium for LMSC cells, 400Å palladium, and 1500Å silver covered both surfaces of the wafer. The back contact included an aluminum reflector of 1 to 2 microns for the LMSC 2 Ω-cm BSR cell. The electron-beam high vacuum deposition used has been the standard in the manufacture of solar cells for space.

3.6.2.2 Photomask Application

A photoresist coat is spun onto both sides of the wafer starting with the back side. A mask designed to provide the desired

contact pattern allows ultraviolet light to reach those areas where contacts are to remain; the U.V. light causes the photoresist to cross-link and become resistant to the developer solution. The unexposed photoresist (on cell active areas) dissolves into developer solutions and a final rinsing insures cleanliness of these areas. Process evolution included insertion of a pre-mask clean, batch processing through development and rinse in cassettes, and determination of usable types of photoresist and their respective application parameters.

Initial attempts at batch processing using a single tank each of developer and rinse did not remove unexposed photoresist cleanly and streaks of incompletely removed p.r. could be seen in the center of wafers where etchback was hindered. Final processing used two progressively cleaner develop baths and three progressively cleaner rinse baths.

3.6.2.3 Etchback of Contact Strike

The first etchback sequence for the Ti-Pd-Ag contacts employed chemical solutions only for removing silver and titanium; the palladium was undercut during the Ti strip and was removed simultaneously. Ammonium hydroxide/hydrogen peroxide removed the silver and a weak solution of hydrofluoric acid removed both the titanium and palladium.

Since the basic silver strip mixture was highly reactive and short-lived, a more controllable anodic etch was developed. "Reverse plating" into a cyanide bath removed the silver; an anodically assisted ammonium bifluoride solution stripped the remaining metals. Variability in this initially successful process appeared suddenly after a number of lots of cells had been processed. Contact metallization was etching away at

different rates so metal was left on one area while grids were etching away on another. The chemical etch was used as a fall-back to process the remainder of the conventional contact cells until the problem was resolved.

Work at the same time progressed on the dielectric wraparound contact strike etchback. Two problems presented themselves: removing the Cr-Pd-Ag contact system used while not damaging the printed dielectric insulation. When the chemical etch was tried, the NH_4OH/H_2O_2 solution did not remove the silver - perhaps some sort of passivation occurred due to the chromium-palladium base layers. Not even aqua regia (3:1 :: HCl : HNO_3) would etch the silver. The anodic CN did remove the silver but all solutions that would etch the chromium also stained the silicon and often removed the photomask as well. These etches also damaged the dielectric.

At this point a mechanical wraparound contact technique replaced the printed dielectric insulation because of the lack of an etch-back process and also because of the increasing projected cost for the cell. The mechanical wraparound cell uses the Ti-Pd-Ag contact system and so posed no additional problems in etchback. Accordingly, one lot of cells was processed with the dielectric wraparound front contact pattern (while the redesigned mask needed was ordered) and received the "N" interconnect bond and weld at the end of fabrication.

At this time, it was seen that the design of the contact mask could have a significant effect on etchback. Difficulty had been seen in etchback on this contact design even when the anodic etch worked properly. Where the grids ran into the main collector bars, the silver on the grids was etching away under-cutting the photomask. The subsequent etch removed the Ti-Pd in this area as well as breaking the grids. This occurrence was

attributed to some field effects associated with the contact pattern design. (The initial cells processed successfully through the anodic etchback, TRW cells, did not have collector bars running across the face of the cell.) The chemical etchback again was used as a fallback to remove the silver with the anodic Ti-Pd etch following.

At the same time, internal work at Spectrolab had added an intermediate, anodic palladium etch; the NH_4HF_2 etch removed the titanium now without anodic assistance.

When the mechanical wraparound cells with the new front contact reached the etchback stage, additional problems were encountered not present in etching back the conventional contacts. The wraparound contact pattern mask did not provide an unbroken border of metal on the perimeter of the wafers. Thus, as the metals were etched away, electrical contact was lost to the areas farthest from the clip attachment, which areas therefore did not etch cleanly. Also, the contact pattern did not have grids running directly into the perimeter so the current path was longer. This lack of a direct electrical path also hindered even plateup of contacts on wafers which had etched back satisfactorily enough to process.

In addition, a back mask pattern designed to facilitate laser scribe alignment on the back of the wafer (cells are scribed from the back) exposed some back contact on parts of the wafer that are scribed off. The evaporated aluminum BSR was being etched away preferentially in the HN_4Cl palladium strip because of its lower electrochemical potential (i.e. the aluminum was acting as a "sacrificial anode" to protect the palladium). Removal of the Pd would not begin until aluminum was undercut from all exposed back contact areas. See Figure 9.

Figure 9

INITIAL DESIGN OF CONTACT MASKS FOR MECHANICAL WRAPAROUND CELLS

ORIGINAL PAGE IS
OF POOR QUALITY

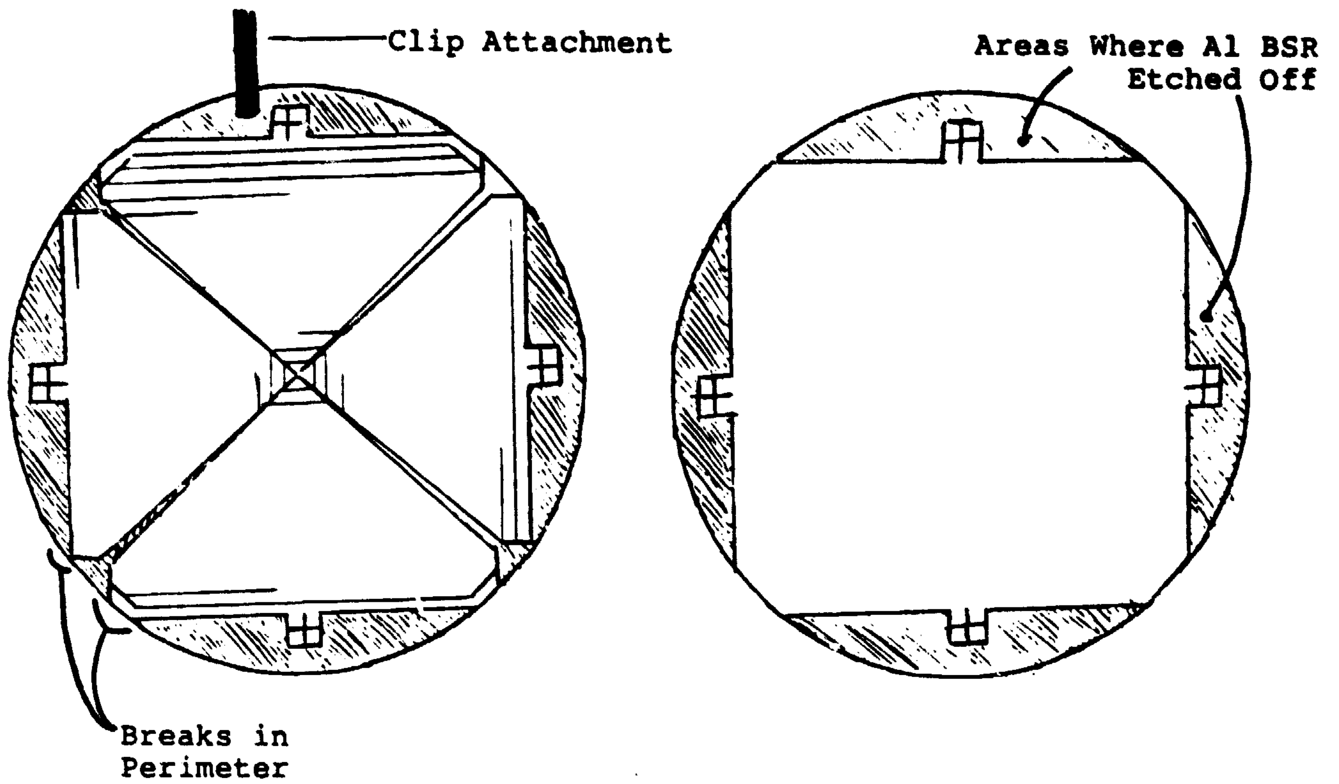

The design of the wraparound contact mask was altered to keep a continuous border on the front of wafers and to utilize full back coverage, and new masks were ordered for photoresist processing. See Figure 10. The cells already processed with the old photomask were given a "touchup" in the four corners to maintain an unbroken perimeter. Cells with exposed back contact had an additional coat of photoresist spun onto the back and hard-baked. Both some smears of the "touchup" compound and some spiderwebbing spun off during the back recoating step were left on the fronts of some cells. These smears protected the contact strike on the front and can be seen as streaks or smears of contact metallization that did not clean off.

The above mentioned steps were in large measure effective in achieving clean etchback. However, the photoresist was not consistently adhering to the contact strike in the cyanide solution, lifting off and allowing etching away of some of the outermost grids. As an interim measure, the NH_4OH/H_2O_2 solution was used to clean off the silver followed by the anodic Pd etch and the Ti etch until photoresist adhesion could be improved. See Figure 11.

3.6.2.4 Photoresist Strip

A proprietary photoresist strip bath manufactured by the supplier of the photoresist in use comprised the photoresist strip. A single soak for two minutes in the heated stripper was followed by a rinse in a cascade rinser. There, the room temperature D.I. water was emulsifying the stripper/ or residue and was not rinsing well. Either ultrasonic cleaning in methyl alcohol directly after the stripper or two successive boiling water rinses improved cleanliness somewhat. The final process evolved used two successively cleaner tanks of heated photoresist stripper and two boiling 1-1-1 trichloroethane rinses followed by an ultrasonic methyl alcohol cleaning and a spin-dry.

Figure 10

REDESIGNED CONTACT MASKS FOR W/A CELLS

ORIGINAL PAGE IS
OF POOR QUALITY

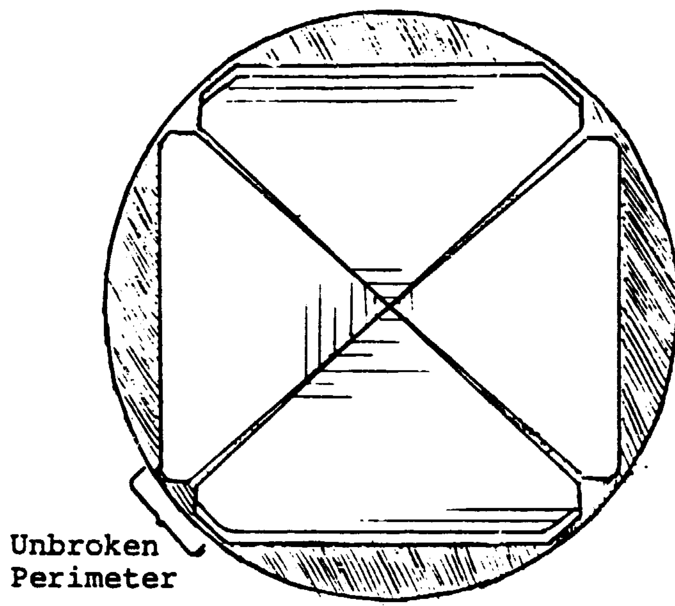

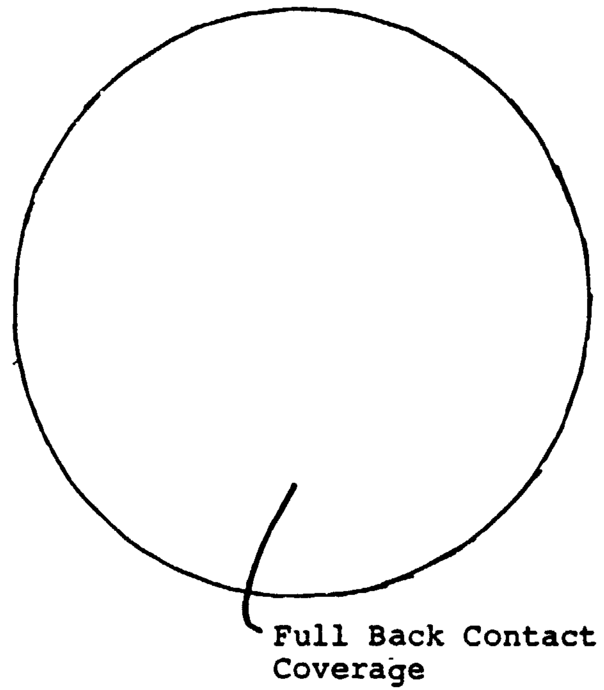

ORIGINAL PAGE IS
OF POOR QUALITY

Figure 11

A) Ag: NH_4OH/H_2O_2

Pd-Ti: HF

B) Ag: CN (Anodic)

Pd-Ti: NH_4HF_2 (Anodic)

C) Ag: CN (Anodic)

Pd: NH_4Cl (Anodic)

Ti: NH_4HF_2

D) Ag: NH_4OH/H_2O_2

Pd: NH_4Cl (Anodic)

Ti: NH_4HF_2

3.6.2.5 Contact Plateup

Initial investigation was performed into pulsed direct current plating to build up contact thickness on small cells as well as into direct current steady state plating. Later work was concentrated on the steady state plating to get a workable process more quickly.

Cells were plated one at a time in a beaker with two silver electrodes and a commercial silver cyanide plating bath. Parameters of plating time and voltage were set to obtain a six micron contact thickness reproducibly. At this time it was noticed that "etch pits" on the active area occasionally resulting from the acid polish etch were plating up full of silver. (The electric field is stronger at the bottom of these pits because of their geometry.) The silver did not adhere well but necessitated rubbing to remove it. The acid polish step was deleted and this active area plating was markedly decreased.

A large tank with a circulating pump and cell holding fixture was set up to plate four cells at once. The 6 x 1½ x ¼ inch electrodes used in the beaker were not of a large enough area to provide a uniform plating thickness on the different cells. Large area electrodes were procured and installed which did provide for even plateup.

When the mechanical wraparound cells were first plated, the lack of a direct current path through the contact metallization was hindering uniform plateup, as it had etchback. The measures taken to improve the etchback also were effective in making the plateup acceptable as well. The voltage and timing parameters were reoptimized for the 2 Ω-cm BSR cell which had a full back contact rather than two "ohmic" contact areas as the 10 Ω-cm BSF cell did.

3.6.2.6 Laser Sizing and Contact Metallization Sinter

Sintering of contact metallization was done in the production facility since large tubes with hydrogen gas flows are not available in the research facility. Even the production tubes would not contain the 3 inch round wafers so the cells were laser sized before sinter.

Initially the wafers were cut to the final size before sinter, which is a two step process. First, two reference cuts from the front were aligned to the front contact pattern. These reference cuts were used to align the laser to the back of the wafer from which the second, final scribing must be done to prevent any electrical degradation. (Precise photomask locating equipment would enable aligning to wafer edges from the back simplifying the scribing.)

This second scribing cuts about 60% into the back of the wafer which is cleaved through the remaining thickness. The cleaving broke through the front contact metallization which was not sintered yet on the first wafers processed and which in some cases was delaminating at the edges during the cleaving. See Figure 12. The narrow corner ohmics on the conventionally contacted cells were sometimes removed by this delamination.

To prevent this occurrence, the sequence of process steps was changed so that the reference cuts occurred before sinter. The contacts were then sintered, dual A/R coating was applied, and the final sizing by the laser became the last step.

Facilities to sinter three inch round or larger wafers would allow all laser sizing to wait until the last step.

Figure 12

ORIGINAL PAGE IS
OF POOR QUALITY

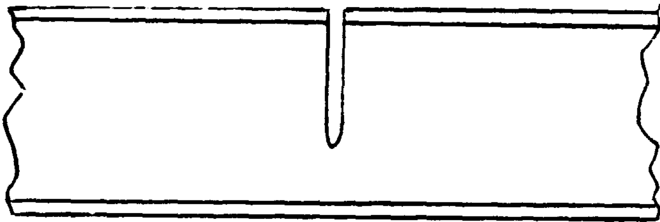

A.

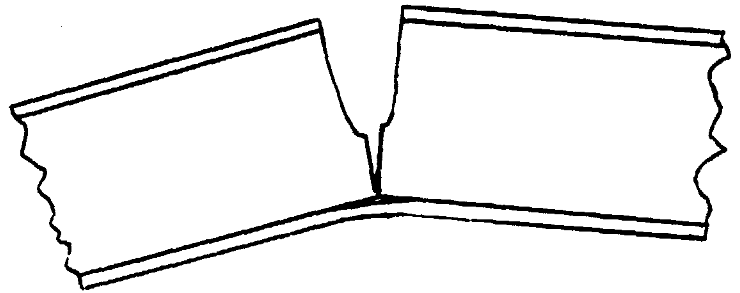

B.

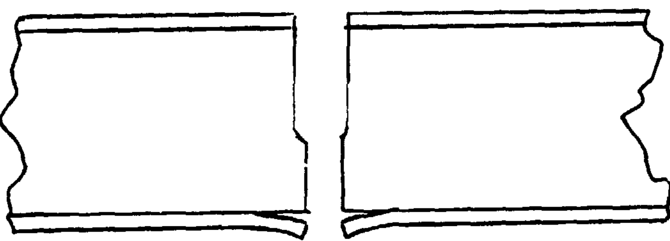

C.

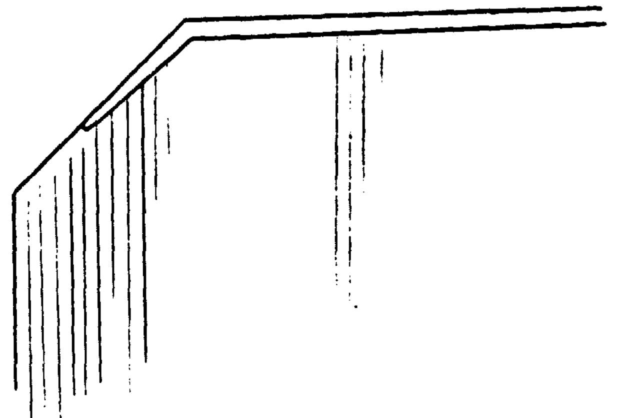

D.

A. Laser Scribed Wafer

B. Break Through Silicon

C. Slight Edge Delamination of Front Contact

D. Partially Missing Corner Ohmic

On the mechanical wraparound cells, a different problem was seen on the corner truncations. A small degree of misalignment on the order of .010 inch or less was enough to scribe off the small collector bars running in from the outermost grids. A large number of cells processed had one or more of these fine collectors missing.

3.7 DUAL ANTIREFLECTIVE COATING

The cells received a dual A/R coating in the production facility. The tooling in the dual A/R machine holds standard wafers with an ohmic along one edge. The three-inch round wafers did not fit well in the tooling and experienced excessive breakage in that process.

Also, tooling to shield the interconnect areas from A/R coating was not available so an aluminum tape was applied to those areas during the coating. Placing and removing this tape accounted for approximately one-half of the breakage in that area.

3.8 MECHANICAL WRAPAROUND BONDING

The first fifteen cells manufactured for examination by LMSC had as a bonding material a sandwich of separate layers of 1 mil modified acrylic - 1 mil kapton - 1 mil modified acrylic. The acrylic used was a Dupont product, the interconnect was 1 mil silver ribbon. These layers were aligned on the bonding buck, one side of the cell at a time, and laminated at 350°F for a short time. The bonding/insulating layers were trimmed close to the cell edge and the silver ribbon was trimmed and wrapped to the front surface. One microspot parallel gap weld was made at each of the four corner wraps.

The front contact of these first cells was designed for the printed dielectric insulation wraparound cell; that photomask

was used until a redesigned mask could be obtained. Since the ribbon interconnect would not wrap around the corner truncations on each side and at the same time pass through the weld pad area on the back of the cell, the corners were truncated in an additional 0.125 inch. The silver ribbon then could wrap around the corners and meet the main collector bars on the front and also be centered on the interconnect areas on the back of the cell. See Figure 13.

The cells thus fabricated had a severe curve shape degradation which was believed to be a shunt. After some investigation into that premise it was noted that the greater amount of truncation done had severed five gridlines on each side of the cell from the main collector bars. The unconnected area contributed a large amount of series resistance as well as acting as a parasitic recombination site, both effects so severe as to bring down short circuit current as well as degrade curve shape. Redesign of the front contact pattern avoided this difficulty.

The remainder of the Lot 1 delivery of cells to LMSC (10 electrical and 10 mechanical samples, to total 25 electrical and 10 mechanical cells) was bonded the same as the first 15 cells. For Lot 2a space-qualified, prelaminated product also manufactured by Dupont was used. Known as Pyralux LF-0111, it utilized layers in the same thicknesses used before. The Pyralux was cut to size and now also pre-tacked to the cell with a heat shoe, with the silver ribbon tacked on top. The tacking eliminated some of the difficulty in obtaining correct positioning since static electricity would cause the loose acrylic-kapton layers to repel one another. Previously the layers also had a tendency to shift around during initial compression in the bonding machine. A larger buck and shoe was used to bond both ribbons simultaneously for Lot 2 cells. The four-corner wraps were spot-welded in the same manner as before.

ORIGINAL PAGE IS
OF POOR QUALITY

Figure 13

LOT 1 DELIVERY OF MECHANICAL WRAPAROUND CELLS

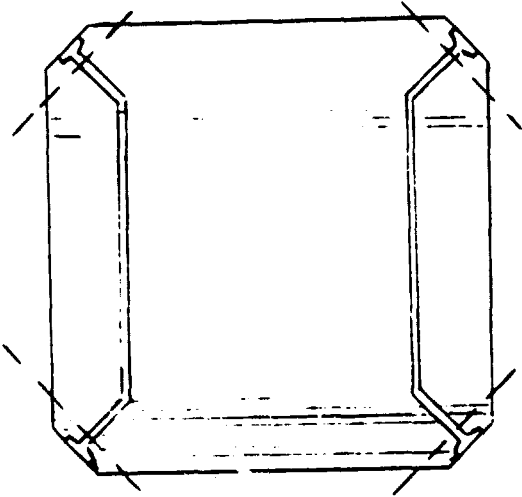

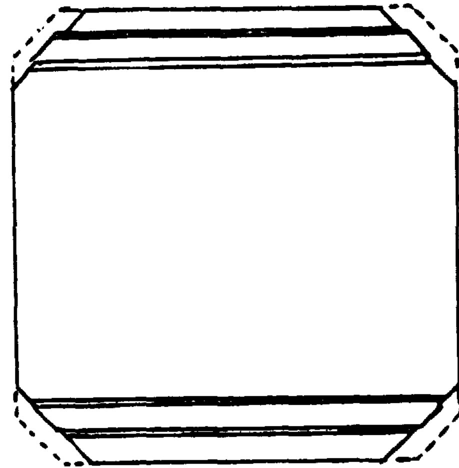

Printed Dielectric Cell
Front Pattern

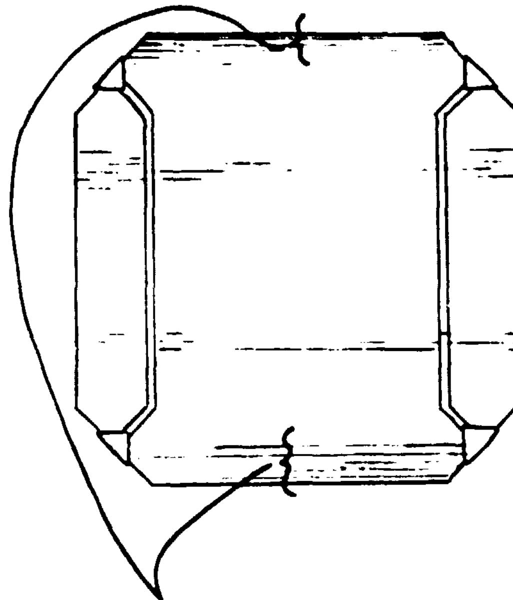

4.0 CELL CHARACTERISTICS

The characteristics of the two cells developed are discussed as to yields in the laboratory, electrical output results, and response to environmental stress testing.

4.1 YIELD DATA

The yield for cell lots manufactured to meet Lot 2 delivery and also following the final process sequences are given in the following sections.

4.1.1 Conventionally Contacted Cell Yield

The total yield for the 180 cells manufactured for Lot 2 delivery is shown in Table 4. These figures are not representative of the process evolved since earlier cells had seen additional process steps that were later deleted.

In Table 5 the yields are given for all cell lots processed with the final process sequences (Lots 6, 7, 8, 9 and 11). Most of the loss was due to wafer breakage with the exception of two process steps. At aluminum paste BSF print and alloy, 50 cells were lost due to insufficient probe voltage. The low voltage is indicative of a low V_{oc} on the completed devices and so the cells were not processed. At etchback, the majority of the lost wafers showed incomplete or excessive removal of the contact metals which made the cells unfit for further processing. Electrical lows were arbitrarily set at below 12% efficiency AM0.

Improvements in yield would result if proper dual A/R tooling was obtained and if the etchback process had been working properly throughout the cell runs. Losses had occurred both to improper etching and as cells were sacrificed to experimentation. Also, identifying the mechanism that causes low open circuit voltages

Table 4

TRW Lots #3, 4, 6, 7, 8, 9, 11

Process	No. of Cells	No. Cells Lost	% Lost	Cause of Loss
Start	418			
NaOH	416	2	0.5	Breakage
Polish		12	2.4	Breakage
Diffuse, V/I	400	4	1.0	Breakage
Print and Fire Al	329	71	17.0	50 Lost to Low Voltage 21 broken
Soda Rub	313	16	3.8	Breakage
PNH Clean	312	1	0.2	Breakage
Heat Treat	306	6	1.4	Breakage
Evaporate Contacts	293	13	3.1	Breakage
Photolithography	255	38	9.1	Breakage
Etch Back	209	46	11.0	Damage to Contact System
Plateup	200	9	2.2	Breakage
Sinter	199	1	0.2	Breakage
A/R	185	14	3.3	Breakage
Laser Scribe	172	13	3.1	Breakage
Electrical Loss	144	28	6.7	Electrical Output $< 12\%\ \eta$

Table 5

TRW Lot # 6, 7, 8, 9 (all), 11

Process	of Cells	No. Cells Lost	% Lost	Cause of Loss
Start	270			
NaOH	270	0	0	
Diffuse, V/I	270	0	0	
Print and Fire Al	212	58	21.5	50 Loss to Low voltage probe 8 broken
Heat Treat	207	5	1.9	Breakage
Soda Rub	202	5	1.9	Breakage
Evaporate Contacts	197	5	1.9	Breakage
Photolithography	184	13	4.8	Breakage
Etch Back	153	31	12.5	Damage to Contact System
Plateup	151	2	0.7	Breakage
Sinter	151	0	0	
A/R	139	12	4.4	Breakage
Laser Scribe	134	5	1.9	Breakage
Electrical Loss	110	24	8.8	Electrical Output <12% η

Total Overall Yield 40.7%

(which might be attributable to other processing such as junction diffusion) might make these occurrences avoidable.

4.1.2 Mechanical Wraparound Contact Cell Yield

Shown in Table 6 are the yield data for the mechanical wraparound cells processed for the Lot 2 delivery to LMSC.

Here again, the main cause of loss was breakage except in the etchback process where a mask redesign was necessary to obtain good results.

Electrical loss was arbitrarily cut off at 10%. Seventeen of these cells or 4.1% were dead shorts.

A large measure of the lower electrical distribution was due to the fact that the laser scribe step was not performed accurately on the corner truncations. The "connector bar" that feeds the side grids into the weld pad was designed to inset .005" from the cell edge. As the cell was rotated 45° on the vacuum chuck to be scribed for the corners, some registry was lost and a large number of cells had their corner connector bars scribed off. Also, the .001" grids were broken in several places on the majority of the cells and the contact system design had not allowed any redundancy in order to increase short circuit current as much as possible.

At the end of Table 6, Lot M5 cells are shown; these cells were reworked from etchback rejects. The wafers had the damaged contact system removed, contact strike re-evaporated, and so on through the processing. Overall yield including these cells is 42.9%.

Table 6

LMSC Lots #M2, M3, M4, M6, M7

Process	No. of Cells	No. Cells Lost	% Lost	Cause of Loss
Start	413			
NaOH	410	3	0.7	Breakage
Diffuse, V/I	406	4	1.0	Breakage
Back Etch	390	16	3.9	Breakage
Evaporate Contacts	382	8	1.9	Breakage
Photolithography	370	12	2.9	Breakage
Etch Back	282	88	21.3	Damage to Contact System
Plateup	264	18	4.4	Breakage
Sinter	263	1	0.2	Breakage
A/R	248	15	3.6	Breakage
Laser Scribe	230	18	4.4	Breakage
Mechanical W/A	212	18	4.4	Breakage
Electrical Loss	167	45	10.9	Electrical Lows <10% n AM0

Total Overall Yield 40.4%

Adding Rework Lot M5: 10 cells 42.9%

Areas for yield improvement are again in the A/R tooling and etchback as well as improving accuracy by more precise laser scribe alignment.

4.2 ELECTRICAL MEASUREMENT DATA

4.2.1 Conventional Contacts

The efficiencies of all cells over 12% efficiency in the 180 cell Lot 2 delivery average 13.0% for 139 cells tested at 28°C, AM0 conditions. The open circuit voltages averaged 601.1 ± 8.5 mV and the average of the short circuit current was 1435.0 ± 32.6 mA. The distribution of cell output for the 180 cells is given in Figure 14. This shows that the distribution peaked at or above 14% efficiency and only the inclusion of low-end cells brought the total efficiency down.

Fill factors averaged .756 for the 139 cells. Average voltage at the maximum power point was 492.7 ± 12.5 mV. Figure 15 is a typical I-V curve.

Thermal alpha measurements done on the 10 Ω-cm BSF/BSR cell type by TRW gave a value of .73-.74 for non-covered cells.

4.2.2 Mechanical Wraparound Cells

The output of the cells produced to meet the Lot 2 delivery of 180 cells averaged 12.1% efficiency at 28°C, AM0 for 168 cells. Open circuit voltages for these cells averaged 581.2 ± 7.4 mV and short circuit current averaged 1273.5 ± 33.3 mA. Figure 16 shows the power distribution for these cells.

The voltage at the maximum power point was 468.1 ± 13.1 mV and the current there was 1187.6 ± 47.6 mA. Coefficients of curve fill factor averaged .757. Figure 17 is a typical I-V curve.

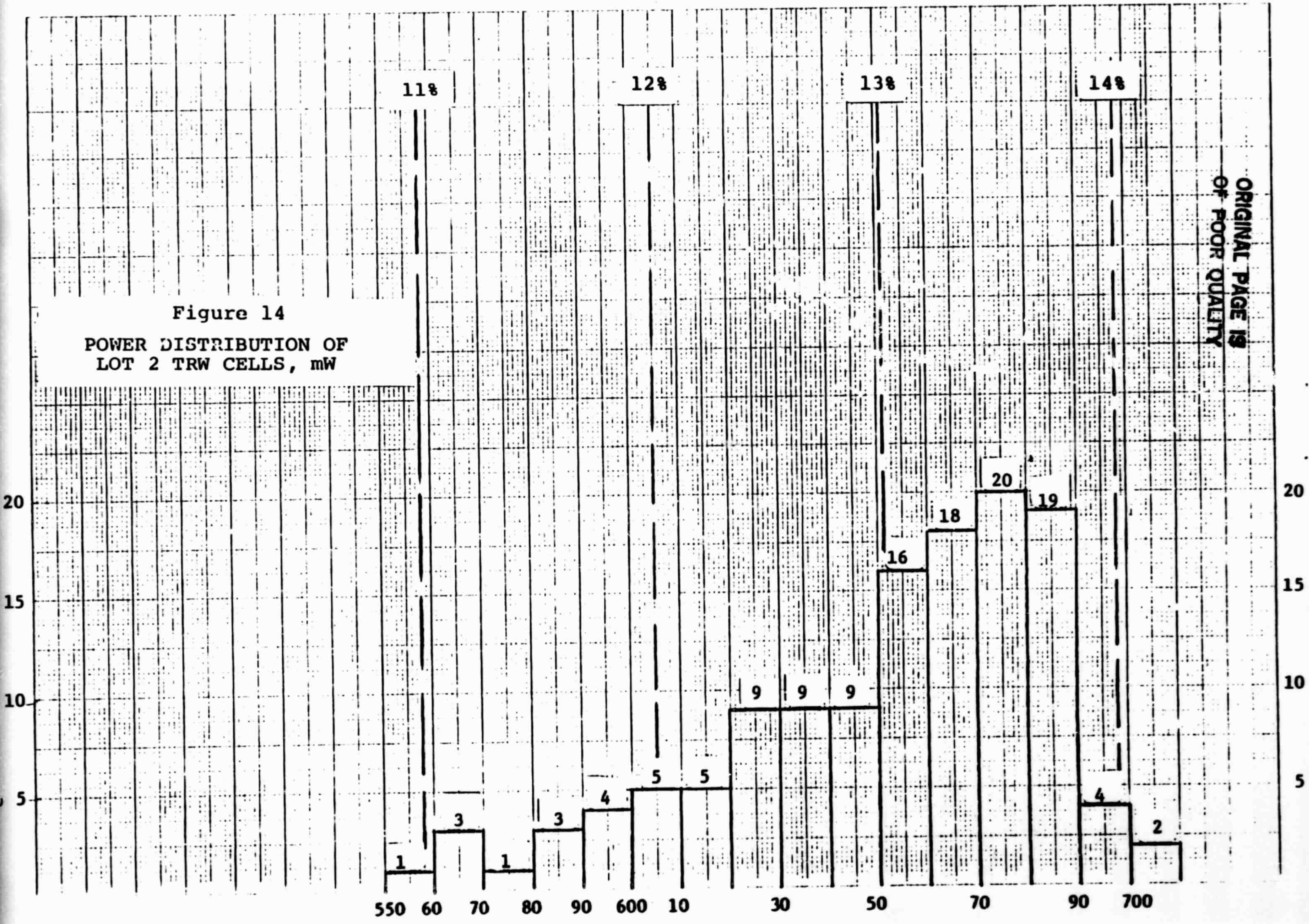

Figure 14

POWER DISTRIBUTION OF LOT 2 TRW CELLS, mW

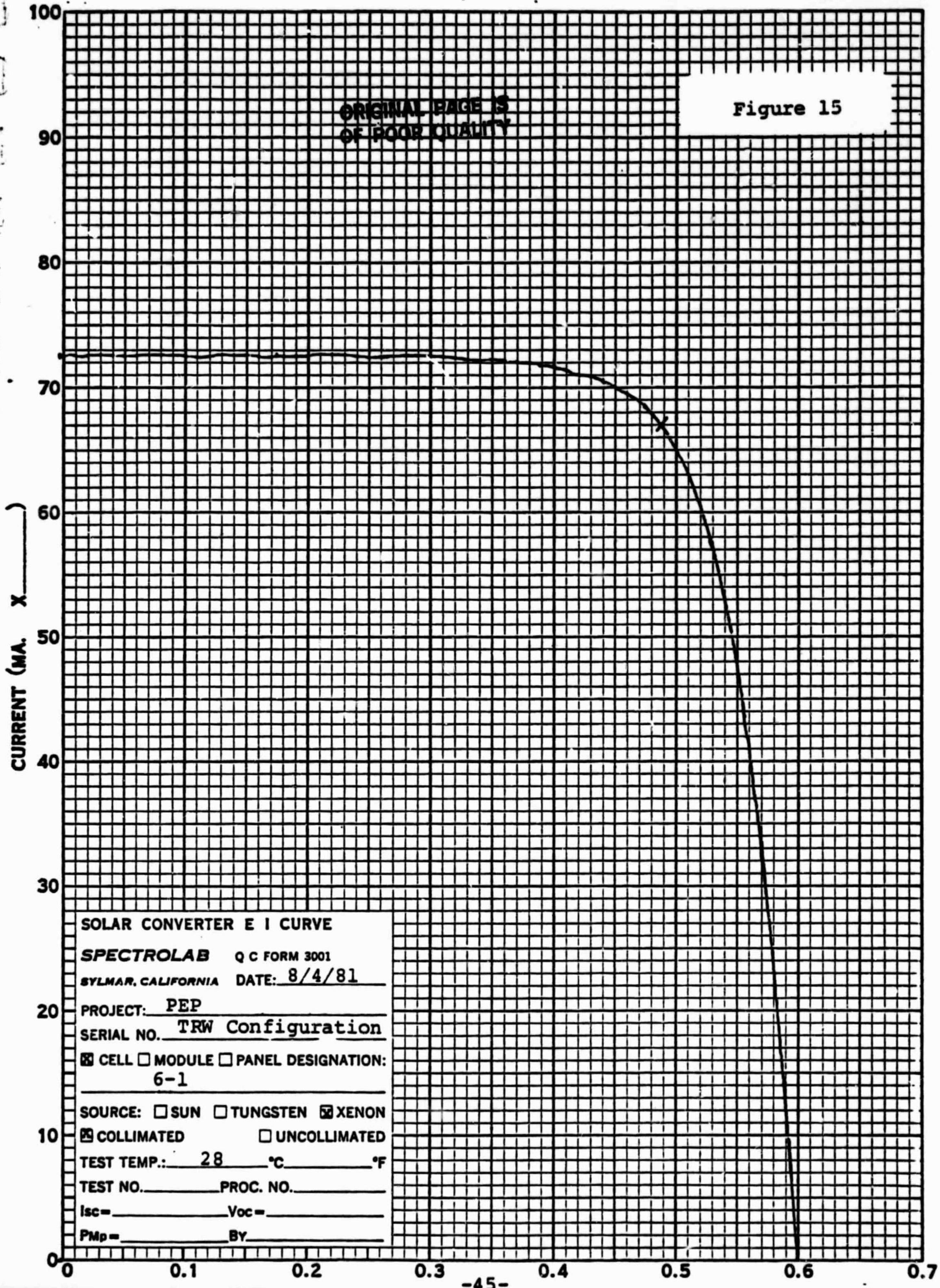

Figure 15
ORIGINAL PAGE IS
OF POOR QUALITY
CURRENT (MA. X
100
90
80
70
60
50
40
30
20
10
0
0
0.1
0.2
0.3
0.4
0.5
0.6
0.7
SOLAR CONVERTER E I CURVE
SPECTROLAB
Q C FORM 3001
SYLMAR, CALIFORNIA
DATE: 8/4/81
PROJECT: PEP
SERIAL NO. TRW Configuration
CELL MODULE PANEL DESIGNATION:
6-1
SOURCE: SUN TUNGSTEN XENON
COLLIMATED
UNCOLLIMATED
TEST TEMP.: 28 °C °F
TEST NO. PROC. NO.
Isc= Voc=
PMp= BY

10 X 10 TO THE CENTIMETER
KEUFFEL & ESSER CO.
46 1523

ORIGINAL PAGE IS
OF POOR QUALITY

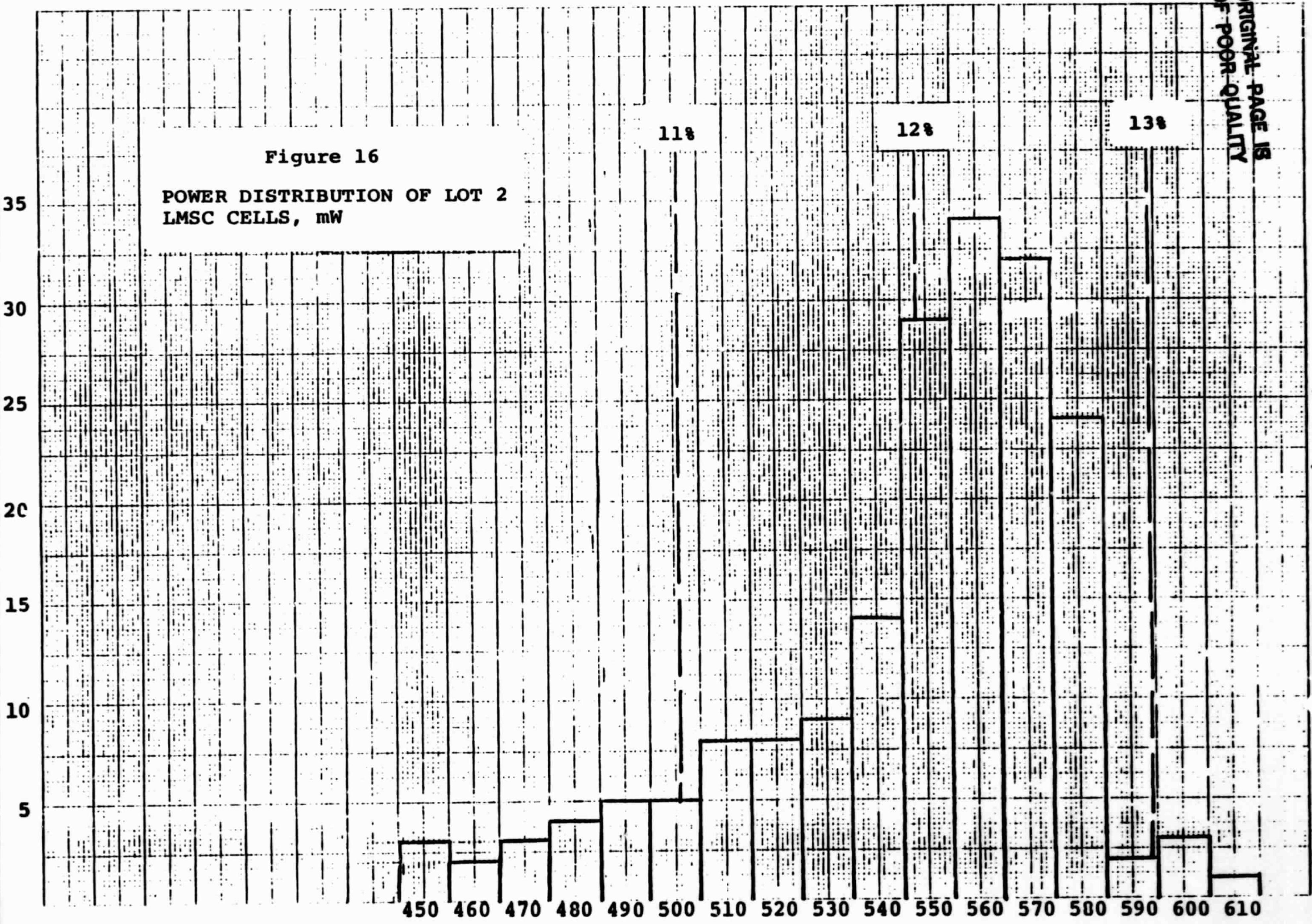

Figure 16

POWER DISTRIBUTION OF LOT 2 LMSC CELLS, mW

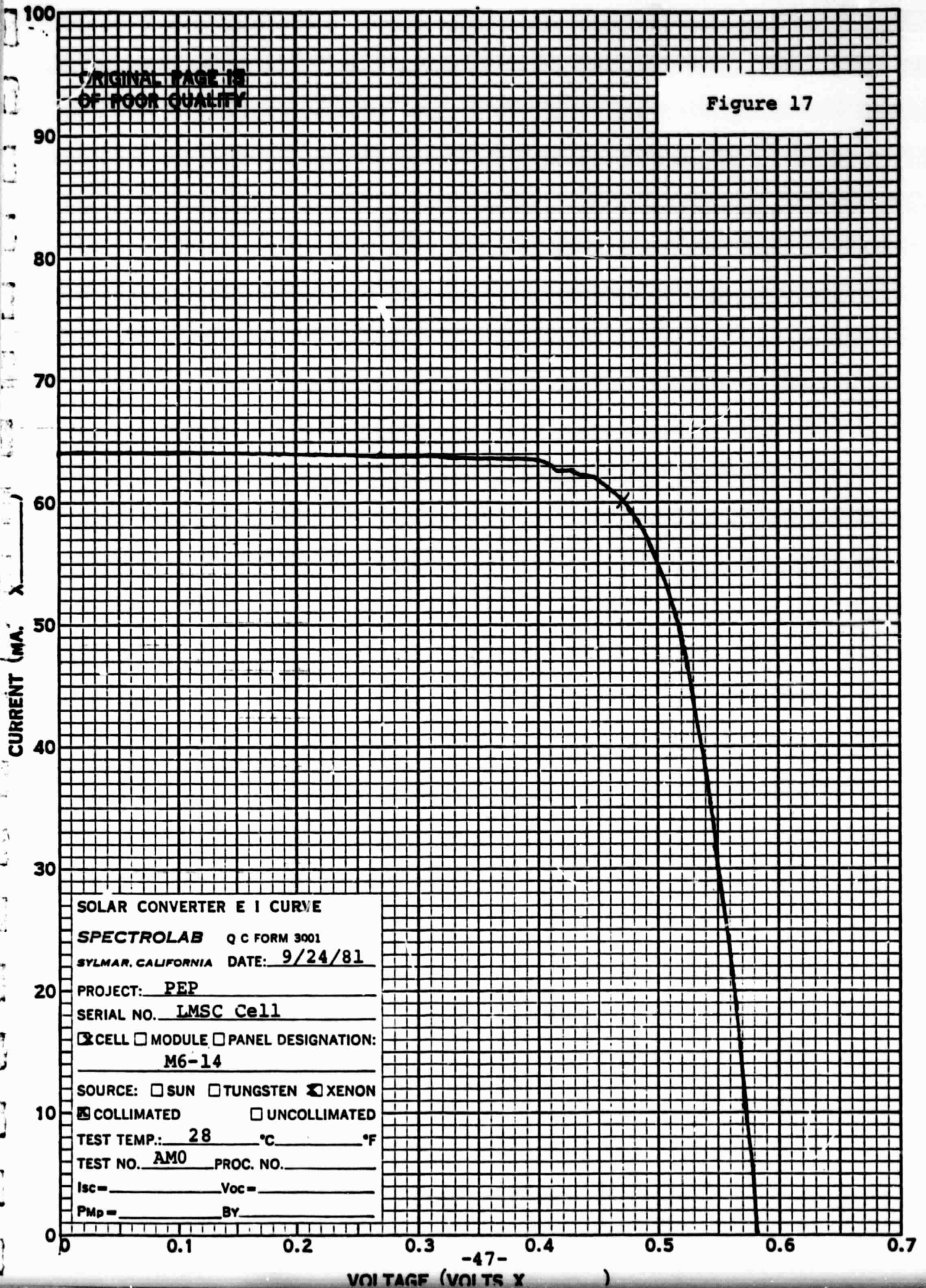
ORIGINAL PAGE IS
OF POOR QUALITY
Figure 17
CURRENT (MA. X)
VOLTAGE (VOLTS X)
100
90
80
70
60
50
40
30
20
10
0
0.1
0.2
0.3
0.4
0.5
0.6
0.7
SOLAR CONVERTER E I CURVE
SPECTROLAB Q C FORM 3001
SYLMAR, CALIFORNIA DATE: 9/24/81
PROJECT: PEP
SERIAL NO. LMSC Cell
CELL MODULE PANEL DESIGNATION:
M6-14
SOURCE: SUN TUNGSTEN XENON
COLLIMATED UNCOLLIMATED
TEST TEMP.: 28 °C °F
TEST NO. AM0 PROC. NO.
Isc= Voc=
PMp= BY

Thermal alpha on these cells was measured by Lockheed at .73 for a cell covered with a fused silica, A/R and UV coated coverslide.

4.3 ELECTRON IRRADIATION TESTING

To facilitate generic cell choice at the beginning of the contract, samples of four cell types were electron irradiated at the NASA-Lewis Research Center Dynametron. Six 2 x 2 cm solar cells of each cell type were tested at the following fluences: zero, 1×10^{13}, 3×10^{13}, 1×10^{14}, and 3×10^{14} 1 MeV electrons/cm^2. Cells were annealed post-irradiation at 60°C for 17 hours. The non-irradiated cells were tested using four different primary standards best matching the spectral response of the cells for simulator set-up. A different set of standards was used for post-irradiation testing since the spectral response of the cells had degraded.

The results of the corrected data are diagrammed in Figure 18.

4.4 THERMAL SHOCK TESTING

In accordance with the document drawn up outlining the TAT-type testing, a sample of five cells of each type was selected from the shipping lot and this sample underwent a ten cycle thermal shock test. Cells were cycled from -196°C (LN_2) to +145°C (hot plate) with a two minute dwell at each temperature once equilibrium had been reached. Post-test electrical testing was performed and cells were inspected for any visible changes.

4.4.1 Conventionally Contacted Cells

Below in Table 7 are the results of the pre-and post-thermal shock electrical testing. No visible signs of degradation were apparent.

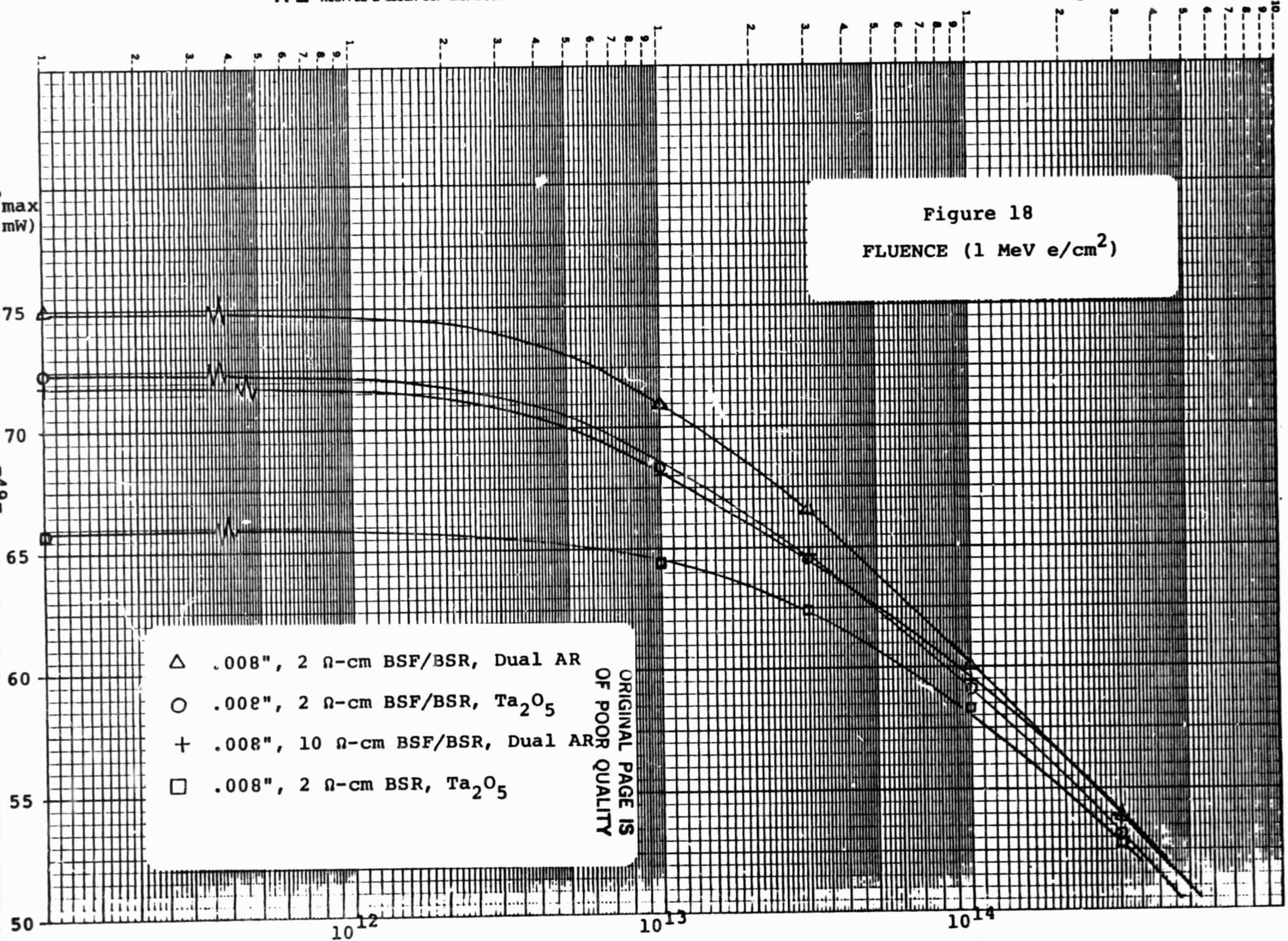

K•E SEMI-LOGARITHMIC 4 CYCLES X 70 DIVISIONS
KEUFFEL & ESSER CO. MADE IN U.S.A.
46 6013
Figure 18
FLUENCE (1 MeV e/cm²)
max
mW)
75
70
65
60
55
50
10¹²
10¹³
10¹⁴
△ .008", 2 Ω-cm BSF/BSR, Dual AR
○ .008", 2 Ω-cm BSF/BSR, Ta₂O₅
+ .008", 10 Ω-cm BSF/BSR, Dual AR
□ .008", 2 Ω-cm BSR, Ta₂O₅
ORIGINAL PAGE IS
OF POOR QUALITY

ORIGINAL PAGE IS
OF POOR QUALITY

Table 7

THERMAL SHOCK TESTING RESULTS
CONVENTIONALLY CONTACTED CELLS

Cell #		V_{oc} mV	I_{sc} mA	V_{mp} mV	I_{mp} mA	P_{mp} mW	CFF	ΔP Change
7-8	Before	600	1440	494	1360	671.8	.777	-0.4%
	After	600	1435	494	1355	669.4	.777	
7-21	Before	603	1440	497	1315	653.6	.753	+0.6%
	After	603	1440	496	1325	657.2	.757	
8-4	Before	602	1465	485	1310	635.4	.720	-0.3%
	After	598	1460	480	1320	633.6	.726	
9-22	Before	605	1460	498	1315	654.9	.741	-1.6%
	After	602	1455	488	1320	644.2	.735	
11-8*	Before	590	1430	480	1300	624.0	.740	+7.9%
	After	587	1420	510	1320	673.2	.808	

Average P_{mp} Change on 5 Cells: +1.2%
Average P_{mp} Change Omitting Cell 11-8: -0.4%
Tested @ AM0, 28°C

*Maximum allowable power degradation per cell: -5%
*Maximum allowable average power degradation: -2%

The most probable cause of the large increase in efficiency of Cell 11-8 was the malfunction of the cell test fixture during the pretest conditions. A set of probes on one side may not have been in contact with the cell so that the reading was taken off one side only, showing higher than actual series resistance.

As is seen, the degradation is within the allowable limits of a standard TAT test.

4.4.2 Mechanical Wraparound Contacted Cells

Below in Table 8 are the results of the pre- and post-thermal shock electrical testing. One cell was broken in handling during the testing.

Three of the four surviving cells experienced excessive maximum power degradation. The mechanism for this degradation was not apparent. Pull testing of the weld joints may indicate a failure there - an extensive optimization of weld schedules was not possible in the time scope of the contract. Also, a failed joint might give the effect of decreased fill factor or increased series resistance that is present.

4.5 HUMIDITY RESISTANCE TESTING

In accordance with documents drawn up for TAT-type testing, humidity resistance tests were performed for each cell type. A sample of five cells of each type were selected from the Lot 2 delivery shipment and subjected to the following tests.

4.5.1 Conventionally Contacted Cells

A five cell sample was placed in humidity storage at 95% RH, 45 ± 5°C for 30 days. Cells were visually inspected before

ORIGINAL PAGE IS
OF POOR QUALITY

Table 8

THERMAL SHOCK TESTING RESULTS
MECHANICAL WRAPAROUND CONTACTED CELLS

Cell #		V_{oc} mV	I_{sc} mA	V_{mp} mV	I_{mp} mA	P_{mp} mW	CFF	ΔP
M3-50	Before	582	1255	462	1210	559.0	.765	+0.9%
	After	582	1255	478	1180	564.0	.772	
M4-1	Before	584	1320	447	1250	555.8	.725	-10.7%
	After	582	1295	436	1145	499.2	.662	
M5-7	Before	575	1300	453	1245	564.0	.755	-18.4%
	After	573	1290	395	1165	460.2	.623	
M6-21	Before	586	1280	477	1230	586.7	.782	
	After			Broken				
M7-16	Before	573	1290	466	1175	547.6	.747	-6.4%
	After	575	1290	442	1160	512.7	.687	

Average P_{mp} Change on 4 Cells: -8.7%
Tested @ AM0, 28°C

Maximum allowable power degradation per cell: -5%
Maximum allowable average power degradation: -2%

and after testing and showed no visible changes. The comparison of pre- and post-electrical testing results are shown in Table 9. As can be seen, the cells did not degrade more than the allowable amounts.

4.5.2 Mechanical Wraparound Contacted Cells

Because of the short time available at the end of the contract after mechanical wraparound cells were fabricated, a humidity storage test of a reasonable length was not possible. A boiling water test was substituted as a test of the cell type, especially the mechanical wraparound bond on the back of the cell.

The comparison of pre- and post-test electrical measurements is shown in Table 10. The degradations are within the allowable amounts.

Table 9

HUMIDITY STORAGE TESTING RESULTS
CONVENTIONALLY CONTACTED CELLS

Cell #		V_{oc} mV	I_{sc} mA	V_{mp} mV	I_{mp} mA	P_{mp} mW	CFF	ΔP
6-5	Before	601	1460	493	1365	672.9	.767	-1.7%
	After	597	1450	488	1355	661.2	.764	
6-6	Before	602	1455	491	1285	630.9	.720	-2.0%
	After	601	1440	485	1275	618.4	.715	
6-7	Before	604	1435	496	1340	664.6	.764	-0.9%
	After	602	1425	495	1330	658.4	.767	
6-10	Before	607	1440	496	1345	667.1	.763	-1.2%
	After	605	1430	492	1340	659.3	.762	
6-12	Before	606	1450	500	1360	680.0	.774	-1.0%
	After	603	1445	497	1355	673.4	.773	

Average P_{mp} Change on 5 Cells: -1.4%
Tested @ AM0, 28°C

Maximum allowable power degradation per cell: -5%
Maximum allowable average power degradation: -2%

ORIGINAL PAGE IS
OF POOR QUALITY

Table 10

HUMIDITY TESTING (BOILING WATER) RESULTS
MECHANICAL WRAPAROUND CONTACTED CELLS

Cell #		V_{oc} mV	I_{sc} mA	V_{mp} mV	I_{mp} mA	P_{mp} mW	CFF	ΔP
M2-6	Before	584	1260	472	1200	566.4	.780	-1.9%
	After	584	1295	477	1165	555.7	.735	
M3-29	Before	584	1260	472	1200	566.4	.769	0.0%
	After	583	1280	476	1190	566.4	.759	
M4-3	Before	585	1305	465	1235	574.3	.752	-1.8%
	After	582	1285	472	1195	564.0	.754	
M6-5	Before	584	1300	468	1195	559.3	.746	-1.9%
	After	581	1295	471	1165	548.7	.729	
M7-45	Before	579	1260	469	1190	558.1	.762	-2.3%
	After	582	1260	468	1165	545.2	.743	

Average P_{mp} Change on 5 Cells: -1.6%
Tested @ AM0, 28°C

Maximum allowable power degradation per cell: -5%
Maximum allowable average power degradation: -2%

ORIGINAL PAGE IS
OF POOR QUALITY

5.0 RECOMMENDATIONS

Among the areas open for further investigation the following stand out:

- The BSR enhancement heat cycle should be studied to determine the parameters that achieve the best back surface reflector.
- The effect of cell processing on the evaporated aluminum BSR can be examined to obtain lower thermal alphas.
- Redesign of both contact patterns vs. junction depth may lead to an increase of short circuit current or of current collection efficiency.
- Accuracy of the laser scribe equipment can be improved by use of photomask fiduciary marks.
- Etchback processing should be refined to function more consistently.
- The cause of degradation of mechanical wraparound cells needs to be identified. An etched mechanical wraparound interconnect may reduce stresses in thermal cycle conditions. Also, a post-bond "cure" of the Pyralux sandwich, as suggested by the manufacturer, may further increase bond strength.

6.0 SUMMARY

Two viable, large area solar cell types have been developed which answer to the need for a reduction in cost per watt for a large array. One cell, the 10 Ω-cm BSF cell, exceeds the 14% AM0 efficiency goal of the contract and also shows a lower thermal alpha (.75 - .76 for a cell filtered with fused silica with a UV rejecting filter) than is common on that cell type. The 2 Ω-cm BSR cell shows promise of attaining the contract goal once some straightforward corrections are made. Also, a low cost wraparound contact technique has been introduced which does not degrade cell performance and is not sensitive to generic cell type or size.

Processes achievable in a mechanized facility have been evolved, reducing much handling at the cell manufacture level.